70-2298

CLAWSER, III, Samuel Matthew, 1943-

THE USE OF THERMOLUMINESCENT DOSIMETERS TO STUDY THE EDGE EFFECT OF PHOTONS IN A BOUNDED MEDIUM.

The University of Oklahoma, Ph.D., 1969
Physics, radiation

University Microfilms, Inc., Ann Arbor, Michigan

THE UNIVERSITY OF OKLAHOMA

GRADUATE COLLEGE

THE USE OF THERMOLUMINESCENT DOSIMETERS TO STUDY THE EDGE EFFECT OF PHOTONS IN A BOUNDED MEDIUM

A DISSERTATION

SUBMITTED TO THE GRADUATE FACULTY

in partial fulfillment of the requirements for the

degree of

DOCTOR OF PHILOSOPHY

BY

SAMUEL MATTHEW CLAWSER, III

Norman, Oklahoma

1969

THE USE OF THERMOLUMINESCENT DOSIMETERS TO STUDY

EDGE EFFECTS FOR PHOTONS IN A BOUNDED MEDIUM

APPROVED BY

Robert J. Nelson

David M. Elliott

Edwin H. Klehr

Helmut J. Fischbach

DISSERTATION COMMITTEE

ACKNOWLEDGEMENTS

The author would like to express his appreciation for the guidance and encouragement of Dr. Robert Y. Nelson and the other members of his doctoral committee: Dr. E. Klehr, Dr. D. Elliott and Dr. H. Fischbeck. A very special thanks is given to Dr. E. M. Smith of the University of Miami for making this research possible. This work was supported by the United States Atomic Energy Commission contract AT-(40-1)-3734.

The methods of this dissertation were made possible with the assistance of many groups and individuals. Thanks to Mr. Al Hancock, Division of Radiation Therapy, Messrs. Donald F. Menker and Gary E. Beck, Division of Radiation Physics at Jackson Memorial Hospital, Miami, Florida and to Messrs. Darrell O. Poole and Charles S. Perry, Division of Radiation Therapy at Mount Sinai, Miami Beach, Florida.

The author is grateful to the U. S. Navy for allowing deferred time to work for his Ph.D. and especially to his family for their continuing encouragement without which this goal would not have been attempted. This work was done in partial fulfillment of the requirements for the degree of Doctor of Philosophy from the University of Oklahoma.

TABLE OF CONTENTS

LIST OF TABLES

LIST OF ILLUSTRATIONS

THE USE OF THERMOLUMINESCENT DOSIMETERS TO STUDY EDGE EFFECTS FOR PHOTONS IN A BOUNDED MEDIUM

CHAPTER I

INTRODUCTION

1.1 Scope

The primary purpose of this dissertation is to experimentally evaluate the perturbation of the dose distribution in a bounded medium for monoenergetic, point-isotropic gamma sources. This study is oriented to the formulation of dose calculations as proposed by the Medical Internal Radiation Dose (MIRD) Committee (MIRD 1968).

The study of effects for photons in bounded media has become necessary because of the increased use of photon sources in finite targets for medical and industrial purposes. Also the currently available methods of dose calculations need experimental information about the approximation to unbounded media.

1.2 Historical Review

For internal point sources, there are three methods of calculating the gamma-ray dose to points within the target (Ellett 1969). One is based on the assumption that there is no change in the number, energy, or angular spectra of gamma-rays between the source and target. This "no absorption" approximation is reasonably valid over distances of a few centimeters for gamma-rays from radium decay products. In this case, the attenuation of the gamma-rays close to the radium source is nearly balanced by the increased dose due to scatter (Meredith *et al*.

1966). Consequently, the development of a better approximation for the dose distribution did not arise from the dosimetric requirements at the site of irradiation but by concern over the total energy absorption in patients.

Since the attenuation of radium gamma-rays cannot be neglected over distances of interest in total body dosimetry, a second method of calculating the gamma-ray dose, which assumes that the gamma-ray energy undergoes exponential absorption between the source and the points of interest, is commonly used. Mayneord initiated studies of this problem (Mayneord 1940; Mayneord and Clarkson, 1944; Mayneord, 1944, 1945) by introducing a point source function characterized by an exponential term containing the "effective" absorption coefficient. The ideas and mathematical techniques developed in his studies were carried over into the dosimetry of other isotopes by Marinelli, Quimby and Hine (1948) in which a generalized system of gamma-ray dosimetry was developed. Marinelli et al. generalized Mayneord's equations by substituting a quantity now known as Γ, the specific gamma-ray constant (I.C.R.U., 1962) for the roentgen exposure rate for radium, and by including uniformly distributed activity through integration over the source volume. However, the integrated geometrical factor is rather arbitrary and often a poor exponential assumption for low-energy photon sources. Although the use of integrated geometrical factors in dose calculations may be justified at energies above several hundred keV; a third method, the exact scattering calculation, often provides better estimates of

the dose at all energies, as well as expresses the dose directly in rads without having to use the roentgen-to-rad conversion factor.

1.3 Methods of Calculating Gamma-Ray Dose

In considering exact methods of predicting the gamma-ray dose, a differential equation which describes the change of photon flux with position in a scattering medium is used. The balance equation of photon number (or photon energy) and direction is called a transport equation and is similar to equations developed by Boltzman to describe gaseous diffusion. The transport equation is applicable to either an infinite medium or bounded regions containing various materials. However, direct numerial integration of the dose transport equation even with the simplest of boundary conditions is not possible on the largest computers. Instead, semi-analytical procedures to provide approximate solutions have been used (Fano et al. 1959). Only the moments and Monte Carlo methods yield more than asymptotic solutions to the transport equation. The moments method gives the spatial moments of the dose distribution rather than an analytical expression for the dose as a function of the spatial variables. From these moments, a series expansion that approximates the values of the dose as a function of the distance from a source is obtained. The main limitation of the moments method is its restriction to gamma-ray diffusion in an infinite homogeneous medium. The Monte Carlo method evaluates the transport equation by means of random sampling and, because each interaction is treated separately, is adaptable to boundary problems. As a result, the objective of this dissertation is to correlate the physical reality of boundary effects for

photons to the Monte Carlo computer calculations and theory.

1.4 Formulation of Study

The Monte Carlo method is commensurate with the theory used by the MIRD Committee to calculate absorbed dose. The edge effect study is related to absorbed dose calculations through the formulation of the MIRD Committee. It is therefore necessary in this section to introduce their nomenclature and theory.

The MIRD dose equations are based on energy absorption rather than air ionization. The unit of absorbed dose as defined by the I.C.R.U. (1956, 1962) is the rad (100 ergs per gram). Specifically, the dose D is equal to the quotient of ΔE_D, the energy imparted by ionizing radiation to matter in a volume element of mass Δm, by Δm (I.C.R.U. 1962):

$$D = \frac{\Delta E_D}{\Delta m} \text{ rad} . \qquad (1)$$

To conveniently describe the emitted energy, Δ_i, for a photon of fractional abundance n_i (corrected for internal conversion) and energy E_i (meV), MIRD (1968) has introduced the equilibrium dose constant

$$\Delta_i = 2.13\, n_i E_i \frac{\text{gram-rads}}{\mu\text{Ci-h}} .$$

Brownell et al. (1968) and Dillman (1969) have a calculated Δ_i for a number of commonly used radionuclides. Table I gives the Δ_i for the radionuclides used in these studies.

Table I. Equilibrium absorbed dose constants.[1]

Radionuclide	Half-life	Principal Energy	Δ_i (g-rad/μCi-h)
Cobalt-57	270 days	123 keV	0.226
Tin-113	115 days	393 keV	0.548
Cesium-137	30 years	662 keV	1.199

[1] Brownell et al. (1968) and Dillman (1969).

The dose D(r) from an internal source is comprised of both scattered and unscattered photons (D_s and D_p respectively).

$$D(r) = D_s(r) + D_p(r)$$

Independent of boundary conditions, the dose from unscattered (primary) radiation can be determined analytically with the use of an exponential term containing the total linear absorption coefficient, $\mu_t(E_i)$, for the primary radiation.

$$D_p(r) = \frac{\tilde{A}\ \Delta i\ \mu_k\ (E_i)\ e^{-\mu_t(E_i)r}}{\rho 4\Pi r^2}\ \text{rad} \qquad (2)$$

where $\tilde{A}$ = Cumulative activity for a point source (uCi-h)

μ_k = Linear energy transfer coefficient for the primary radiation (cm^{-1})

ρ = Density of target ($g\text{-}cm^{-3}$)

r = Distance from source to point of interest (cm).

However, to include dose calculations for scattering media, the term energy transfer buildup factor, B, was introduced. B is a function of both the initial energy E_i, the distance from the source r, and the source configuration and boundary conditions u,

$$B(E_i,r,u) = \frac{D(r)}{D_p(r)}$$

$$= 1 + \frac{D_s(r)}{D_p(r)} \quad .$$

Therefore, the total absorbed dose function for a point source becomes

$$D(r) = \tilde{A}\,\Delta_i \frac{\mu_k}{\rho} \frac{e^{-\mu_t r}}{4\pi r^2} B \text{ rad} . \qquad (3)$$

Equation (3) is the fundamental absorbed dose equation which is often used to analytically calculate the energy absorption buildup factor, B. However, implicit in Equation (3) are the restrictions of a point isotropic source and homogeneous unbounded media. It is a combination of both the second method (attenuation) and the third method (exact scatter) for calculating gamma-ray absorbed dose. To use only the exact scatter method new terms must be defined.

Absorbed fractions are useful for calculating the average gamma-ray energy absorbed by a volume containing radioactivity. The absorbed fraction is defined as the ratio of the energy absorbed in the target to the energy emitted by the source.

$$\phi = \frac{\text{energy absorbed}}{\text{energy emitted}} \qquad (4)$$

It is a function of the photon energy E_i, the mass of the absorbing volume m, and the geometry of the source and absorber. Using this term, the average dose $\bar{D}$ received by a target of mass m from a point source of cumulative activity $\tilde{A}$ is

$$\bar{D} = \frac{\tilde{A}}{M} \phi_i \Delta_i \text{ rad} . \qquad (5)$$

For uniformly distributed activity in which the source volume is the same as the target volume, the average dose $\bar{D}$ is

$$\bar{D} = \tilde{C} \sum_i \phi_i \Delta_i \text{ rad} \qquad (6)$$

where $\tilde{C}$ is the cumulative concentration of activity in μCi-h/g.

To extend the idea of absorbed fractions to include the dose at a point, the specific absorbed fraction, Φ, was introduced by Loevinger and Berman (1968). Φ is the fraction of the emitted energy absorbed per gram of absorbing material at the point of interest. The absorbed dose equation is then expressed as,

$$D = \tilde{A} \sum_i \Delta_i \Phi_i \text{ rad} . \qquad (7)$$

Unlike the absorbed fraction, ϕ, which is dimensionless, the specific absorbed fraction, Φ, has the units per gram (g^{-1}). By definition, Φ is bounded by zero and one, but Φ can have any positive value depending on the amount of absorption per gram of the target region. It is, however, a useful formalism for presenting results of exact scattering calculations, and therefore will be the factor which is used to describe the edge effect for photons in a bounded medium.

CHAPTER II

THERMOLUMINESCENT DOSIMETRY

2.1 Historical Review

The phenomenon of thermoluminescence was first reported as far back as the seventeenth century by the physicist Boyle, while he was studying the properties of diamonds. From that time through the early 1900's virtually no progress was made toward the practical use of thermoluminescence as a dosimetry system. Finally, in 1947, Dr. F. Daniels of the University of Wisconsin visualized the possibilities of this phenomenon for practical dosimetry and initiated the first program of research dedicated to study in this field. Between 1950 and 1960 there was a brief lag in the research of thermoluminescence. In 1960 new interest was stimulated through research in this field due to the efforts of Dr. John R. Cameron of the Radiology Department at the University of Wisconsin. Today, as a result of extensive research in the applications of thermoluminescent detector (TLD) systems, especially for clinical dosimetry and health physics applications, there are a dozen companies involved in the manufacture of these systems. Each of these systems has its own particular capabilities. The current development and future applications of TLD systems are constantly increasing. There are many references available which elaborate on the details of the mechanics and theory of thermoluminescence detection, as well as the historical development of the field (Attix, 1967: Cameron, 1967, 1968; Lin, 1968).

2.2 Fundamental Theory

Thermoluminescent dosimetry has added an additional versatility for measuring radiation. Several disciplines of science are finding useful applications for TLD systems.

The use of a thermoluminescent detector system made this research feasible. The TLD system used in this research was a Harshaw TLD Analyzer Model 2000 and Harshaw LiF-100 extruded rod detectors (1.4 mm x 1.4 mm x 7 mm). (See Figures 1 and 2 respectively). The experimental objectives could only be obtained by a detection system which would not appreciably distort the radiation field yet sensitive enough to quantitatively gain information about the absorbed dose. The physical dimensions of a Lithium Flouride thermoluminescent crystal detector is a good approximation to the ideal "Point Detector" in addition to processing approximate tissue equivalence. The small physical dimensions that can be obtained with the TL crystal material of milligram quantities is one of the most promising characteristics of this detection system. Endres (1965) has shown that essentially, the TLD does not interfere or physically disturb the radiation field which is being measured if it is at least two cm from the source. The tissue equivalence approximation is based on the effective atomic number ($\bar{Z}$) of the compound: $\bar{Z}_{Lif} = 7.14$; $\bar{Z}_{tissue} = 7.42$; $\bar{Z}_{air} = 7.64$. Cluchet and Joffre (1967) have shown that the sensitivity of LiF relative to tissue is proportional, and therefore can be considered "tissue equivalent". These two properties of LiF-100 were necessary for good results

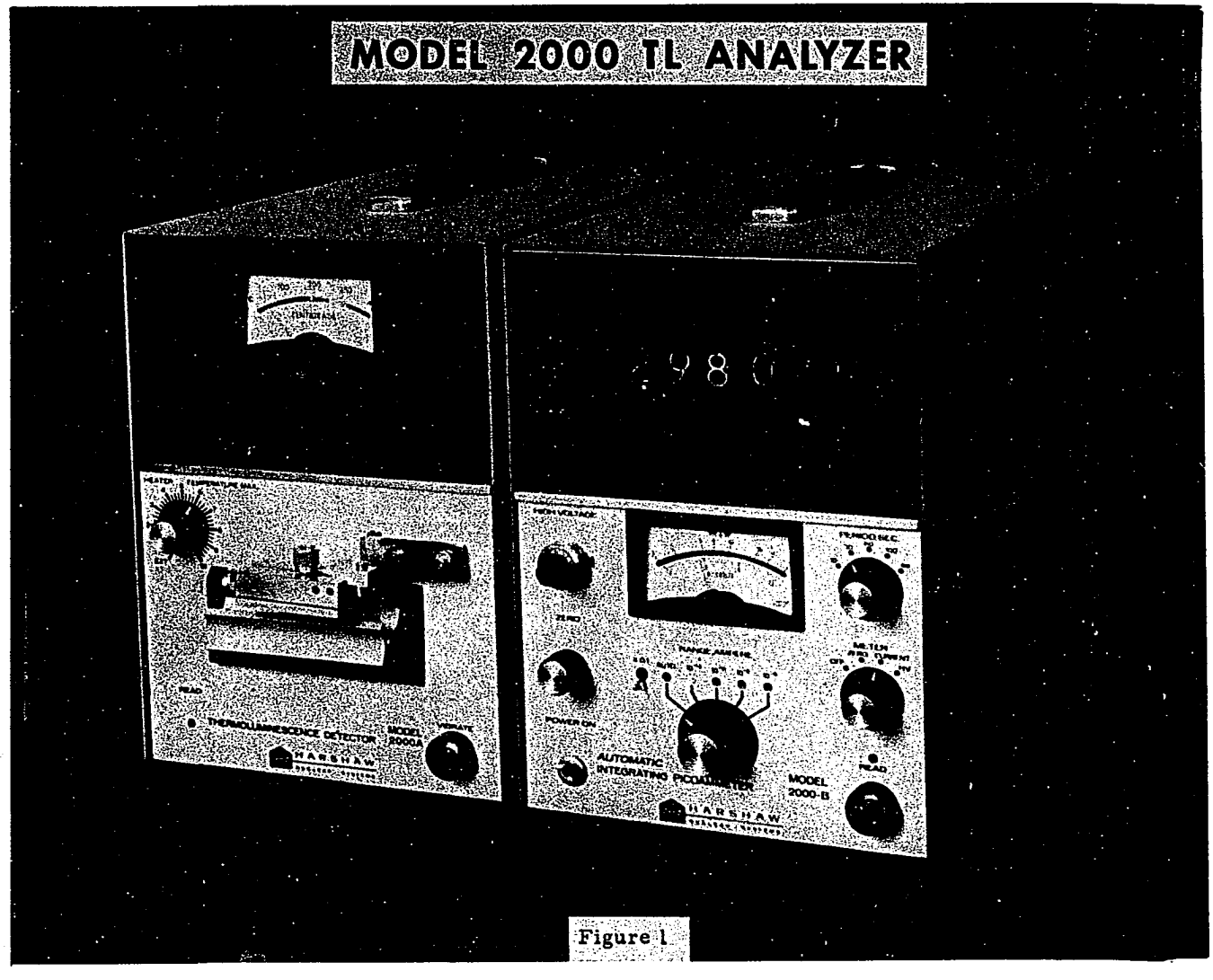
MODEL 2000 TL ANALYZER
THERMOLUMINESCENCE DETECTOR MODEL 2000A
HARSHAW
AUTOMATIC INTEGRATING PICOAMMETER
MODEL 2000-B
HARSHAW

Figure 1

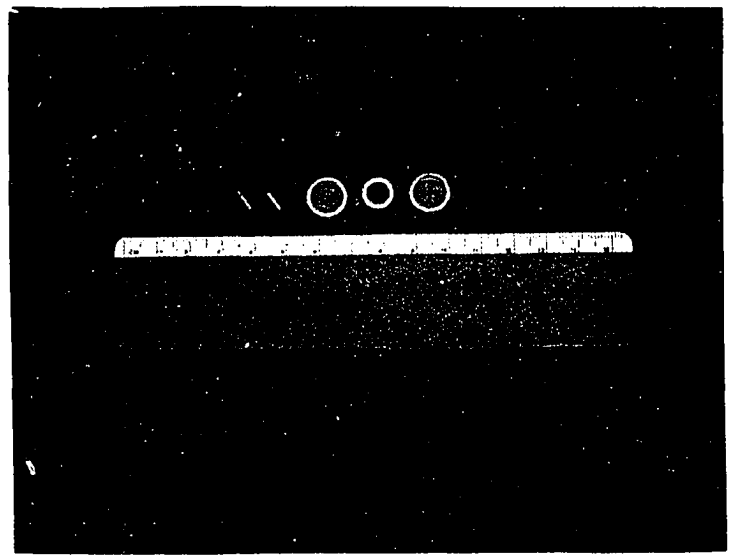

Figure 2. LiF-100 Extruded Rod Detectors (1.4 mm x 1.4 mm x 7 mm) and Plastic Mounted Discs (1.27 cm diam. x 0.635 cm depth) for Sources.

in this study; however, many other characteristic properties of TL systems were also useful for dosimetry application.

Fortunately, lithium fluoride is one of the most widely used thermoluminescent dosimeter material. Its desirable radiation dosimetry properties have become well documented over the last eight years and include: wide exposure measurements range (several mR to greater than 10^5R) (Palmer, 1966; Suntharalingam et al., 1967; Hall, 1966); exposure rate independence to greater than 10" rads per second (Karzmark et al., 1954; Tochilin and Goldstein, 1965); essential energy independence (Cameron et al., 1961; Jones et al., 1966); long term response retention (less than 5 per cent loss of response at room temperature for 12 weeks) (Suntharalingam, 1968); and can be used to accurately measure the response of gamma-rays (Cameron, 1967). Cameron, Kenney, and Suntharalingam (1968) have published the first text book in thermoluminescent dosimetry which gives most recent developments, and progress reports, made available by Harshaw Chemical Co., are released periodically from the University of Wisconsin.

The basic mechanism of thermoluminescent dosimetry is the emission of light from heated, crystalline solids that have previously been exposed to radiation. The light output is proportional to the absorbed radiation energy (rad) and under controlled, reproducible conditions it can be used as a comparison with radiation exposure (roentgen). Although other crystals exhibit this property, today the materials most commonly used commercially are lithium fluoride, calcium sulfate, calcium fluoride and lithium borate. The current theory of the TL system

relates the luminescence (light) from the irradiated substance (detector) which has been thermally excited (heated), to the presence of impurities in the material. These impurities provide trap centers in the energy bands capable of attracting and binding electrons (or holes) released from the ground state by ionizing radiation. Manufacturers are able to produce such trap irregularities by dropping the base crystalline material with various compounds (Jones et al., 1964). When heat is applied to the crystal, the bound electrons (or holes) in the trap centers receive enough kinetic energy to reach the conduction or valence band; however, finally recombining with a metastable hole (or the original electron) trap, thereby emitting light. The emitted light or luminescence is then detected by the photomultiplier tube of a TL analyzer which electrically registers the response. The analyzer recorded response can be then correlated to energy deposition.

The correlation between the emitted light and the energy deposited in the detector material can be explained in the first approximation by a simple first-order-kinetics (i.e. no retrapping effects) model developed by Randall and Wilkins (1945). In their mathematical model for thermoluminescence and long-period phosphorescence, it is required that each electron trap was a distinct, self-sufficient entity. Assuming no retrapping of thermally released carriers, they postulated that for the trapped electrons having a Maxwellian distribution of thermal energies, the probability of an electron escaping per unit of time from a trap of depth E eV at temperature T °K, is given by

$$p = -\frac{1}{n}\frac{dn}{dt} = s \exp(-E/kT) \qquad (8)$$

where n is the number of traps, k is Boltzman's constant, and s is the frequency factor for crystal lattice vibrations; it is almost a constant ($\sim 10^{10} sec^{-1}$), varying only slightly with temperature. Since there are several different trap depth groups, the total escape rate is a summation of the individual rates. Also, since the electrons (or holes) escape from their trap centers to the conduction (or valence) band by application of sufficient heat, in order to maintain long-term retention of dose response at ambient temperatures, these trap centers cannot be too shallow. Cameron et al. (1967) and Braunlich et al. (1967) proposed more detailed mathematical models for thermoluminescence, but all these can be generalized to fit the first approximation model of Randall-Wilkins. That the concepts of the Randall and Wilkins, model do not allow a rigorous treatment of the entire phenomenon of TL with LiF is obvious. But, if their model is used for relating the factors of trap depth, phosphorescence time, and temperature within the rationale of an isolated luminescence center, then it can be used to describe basic operational thermoluminescence.

The most generally used method of studying the energy distribution of electron traps is by means of a "glow curve" (See Figure 3). This is a plot of the light output versus the temperature during the heating process. The temperature increases at a constant rate with time. The resulting glow curve has one or more peaks corresponding to the energy

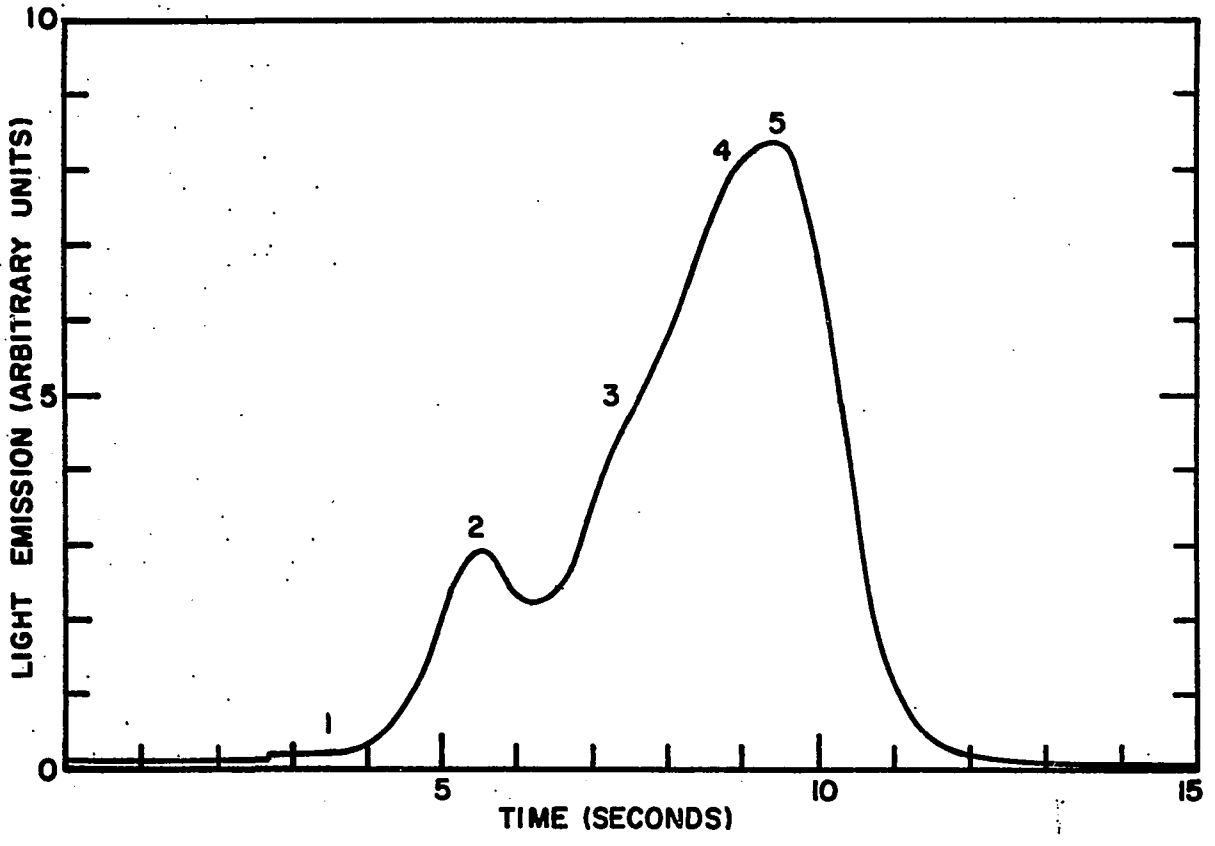

Figure 3. Typical Glow Curve of LiF After Annealing One Hour at 400°C.

levels of the trapped electrons. A higher temperature would provide the necessary kinetic energy for escape of the more deeply bound electron (or hole). Furthermore, since the heating rate is kept constant, the height of the peaks will give an approximate indication of the relative number of electrons trapped at each of the energy levels.

A useful expression to correlate glow-peak temperature with isothermal phosphorescence decay can be derived from Equation (8). Now the maximum intensity of the glow occurs somewhat below that temperature at which the probability of an electron escaping from a trap is 1 per second. Therefore, Equation (8) becomes

$$1 = s \exp[- E/kT_g\{1 + f(s,\beta)\}]$$

or

$$E = T_g \{1 + f(s,\beta)\} k \log s,$$

where T_g = temperature of the glow peak; β = rate of warming (dT/dt); $f(s,\beta)$ = functional change from true exponential decay which is much less than one. For a constant heating rate where $\beta = 0$,

$$E = T_g k \log s . \qquad (9)$$

Integration of Equation (8) from the initial number of filled traps n_o at $t = o$, to n filled traps to $t = t$ gives

$$\log \left(\frac{n}{n_o}\right) = - st \exp(- E/kT) . \qquad (10)$$

Substituting E from Equation (9) into Equation (10), the result is

$$\log \left(\frac{n_o}{n}\right) = ts^{(1-T_g/T)} \quad . \qquad (11)$$

This equation can be used to analytically describe the glow curve and related peaks.

Zimmerman et al. (1967) have identified 5 peaks in the glow curve a lithium fluoride phosphor. After irradiation, peaks 1 through 5 decay at room temperature with the following approximate half-lives: 5 min., 10 hr., 0.5 hr., 7 yr., and 80 yr., respectively. Consequently, peaks 4 and 5 are most suitable for use in dosimetry measurement. Peaks 1, 2 and 3 can be significantly reduced by proper annealing procedures which will be described next.

2.3 Operational Procedures

The major limitation on the precision attainable with thermoluminescent dosimetry has been the presence of the low temperature glow peaks. Like the dosimetry peak 5, these peaks are produced as a result of incident ionizing radiation; however, they are also produced by the emptying of charge carriers from shallow traps, and decay significantly at ambient temperatures. Thus, with the common technique employed for TL readout, a given radiation dose produces a signal which is strongly dependent on the short-term storage time of the phosphor after irradiation.

Therefore, theoretical considerations dictate that before the LiF crystal detector (Harshaw LiF-100 crystals in this research) can be exposed, all energy trap levels should be emptied equally each time. To accomplish this reference condition, the Harshaw Chemical Company (1968) has recommended two pre-irradiation annealing procedures: 1) one hour at 400° C followed by 24 hours at 80° C for low dose experiments, and 2) one hour at 400° C followed by 2 hours at 100° C for less sensitive experimental exposures. The difference in the second pre-irradiation annealing procedure can be explained by noting that the one hour at 400° C empties the trap levels for the dosimetry peaks 4 and 5, whereas the second temperature empties the levels for the low temperature peaks 1, 2 and 3. Under the low dose exposure condition, the room light absorbed by peaks 1, 2 and 3 could increase their magnitude enough to mask the primary peaks 4 and 5. Good precision and reproducible results would not then be possible. As an additional precaution, a recommended post-irradiation annealing of ten minutes at 100° C is also used to reduce the effect of the "light peaks" 1, 2 and 3 which may have occurred during irradiation and before readout. For the work in this dissertation, the longer pre-irradiation annealing cycle was used for greater reproducibility at low levels of exposure (Karzmark et al., 1966). Harris and Jackson (1968) and Carlsson (1969) have published the most recent analysis of the thermal history for TLD LiF, but their results are not significantly different from the recommended Harshaw procedures. All annealing procedures were conducted in a type-F10500 Thermolyne Electric Furnace from the Thermolyne Corporation, Dubuque, Iowa.

Besides annealing, proper handling procedures were necessary. The LiF rods were cleaned in a methanol rinse before and after use; and periodically with trichloroethylene because any contamination on the surface of a rod would alter its response during irradiation and its luminescence during read-out. The heating planchets in which the rods were placed for read-out by the Harshaw Model 2000A Detector System were also periodically boiled in trichloroethylene for ten minutes followed by a quick methanol rinse. This procedure cleaned the planchets of contamination and increased their useful lifetime. The geometry of the heating planchets was designed to fit exactly the dimensions of the LiF rods in order to attain good heat conduction for increased sensitivity (Burch 1968). As recommended by Harshaw Chemical Company, a nitrogen purge of ~4 liters per minute was used to minimize the dark current ($\sim 10^{-12}$A) of the TLD system which was operating at 900 volts. The nitrogen purge also prevented scorching of the sample planchets. All procedures were carefully standardized for better reproducibility. Other details that were taken into consideration were specific for the Harshaw Model 2000 TL Analyzer System, and are listed in the system operational manual under the new additional section 2-15 which was written by the author of this dissertation.

2.4 Calibration Study

To measure true dose (rad) there are only three currently used standards: calorimetry, chemical dosimetry, and free-air ionization

chamber. Of these, calorimetry is the only absolute measure of absorbed energy (I.C.R.U. 1962). TL dosimeters are not absolute radiation detectors. Consequently, all TLD systems must be calibrated by exposing the dosimeter to known amounts of radiation.

Unfortunately, practical methods of calibration were developed before the concepts of units were well defined. In addition to the confusion of universally accepted units, the practical use of radiation measuring devices complicate results even further (I.C.R.U. 1959, 1962). Practical standards that were used measured the ability of a photon to produce ionization in air (roentgen). Recently the roentgen has been redefined as the unit of exposure rather than dose (energy deposition in matter). "The special unit of exposure is the roentgen, R, where 1R = 2.58×10^{-4} Coulomb per kg (air)" (I.C.R.U., 1962). It is possible to convert exposure to absorbed dose in rads provided charged particle equilibrium exists and the spectral distribution of the photons at the location of interest is known.

Charged particle equilibrium has been defined in several texts (Johns, 1964; Hine and Brownell, 1964). When a photon strikes an object, it ionizes that material. The secondary charged particles (electrons) which are consequently set in motion, travel a certain distance (range) which is a function of the photon energy and the medium. If all the secondary electrons created by the photons are stopped in the irradiated medium, then the complete absorbed dose of the photon is produced. However, if as many electrons come to rest as are set into

motion in the medium, then the same effect results. The amount of material required to achieve this charged particle equilibrium is defined as the buildup material.

Under the conditions of charged particle equilibrium, the dose in a medium from a given exposure of gamma-radiation is proportional to the energy absorbed in air per roentgen, and to the ratio of the mass energy-absorption coefficients of the medium and air (μ_{en}/ρ). This ratio varies with photon energy which is, also, in a scattering medium a function of position.

The energy transferred to air from a 1 roentgen exposure is $86.\bar{9}$ ergs/g (I.C.R.U., 1962), the line above the 9 indicating that it is not a significant number. This conversion factor is based on the assumption that 33.7 eV are required to produce one ion pair, and that this energy quantity is independent of both the gamma-ray and secondary electron energy spectrum. Under these and charged particle equilibrium conditions, the energy absorbed per gram from a exposure of R roentgens by gamma-rays of energy E is

$$D_{medium} = f(E)\ R\ (rad) \tag{12}$$

where

$$f(E) = 0.869\ \frac{\left(\frac{\mu_{en}(E)}{\rho}\right)_{medium}}{\left(\frac{\mu_{en}(E)}{\rho}\right)_{air}}\ \left(\frac{rad}{roentgen}\right) . \tag{13}$$

The roentgen to rad conversion based on only initial energy is at best an approximation. Tables of f(E) as a function of photon energy for various tissues have been published by the I.C.R.U. (1962). Usually, sufficient data on the photon spectral distribution are not available, and often the assumption is made that the energy-absorption coefficient does not change much with energy. In tissue and tissue-equivalent material, this assumption is a reasonable approximation since the maximum variation of f(E) is only 10 per cent for photons between 0.01 and 10 MeV (Ellett, 1969). The LiF conversion factors used for the energies in this research were obtained from publications of Ellett (1969) for the low energy sources, and Attix (1969) for colbalt-60 source.

Two methods of calibration were used. Each was conducted at a different hospital facility for the purpose of crosschecking the accuracy of the results. The first calibration technique was conducted at Jackson Memorial Hospital, Miami, Florida. It consisted of exposing LiF rods, which were enclosed by sufficient buildup material (5mm of lucite) for Co-60 radiation (Barnard, 1964). The radiation source was a Pickard Therapeutic Unit which had been calibrated with a NBS calibrated Victoreen chamber. Dose values were computed using the f factor for water medium, correcting for backscatter and buildup material attenuation. The second calibration was conducted at Mount Sinai Hospital, Miami Beach, Florida, using a Framer-Balwin ionization chamber that had a reported accuracy of ± 1 per cent of the measured value within the range of 5R to 120R (calibrated at the National Physical Laboratory NPL,

London, England). The procedure followed in this calibration was similar to the first technique except the LiF rods were inserted into a water phantom (30cm x 30cm) 5cm below the surface. The absorbed dose was determined by following exactly the method prescribed in the "Codes of Practice for Radiation Dosimetry" by the Hospital Physicists' Association, 6 Paddington Street, London W.I. (1964). This method used the f factor for water medium corrected for depth. The good correlation of these two techniques is shown in Figure 4. These calibration procedures were repeated periodically during the entire period of research. They were also carried out after replacement of heating planchets, because reports indicated a decrease in sensitivity of up to 15 per cent between new and tarnished planchets (Cox, 1968). All reading and handling procedures used during calibration were followed exactly during measurements.

During read-out with the TLD system, the current proven method of obtaining a meaningful TL response which can be correlated to radiation exposure is (Cox, 1968):

1) Read irradiated thermoluminescence crystal sample;
2) Cool sample to the initial temperature used in step one;
3) Re-read TL sample;
4) Correlate the algebraic difference of the above two readings to the appropriate dose determination.

This procedure minimizes the undesired variations resulting from non-radiation induced thermoluminescence (NRI-TL) and permits the measurement of a zero response (the algebraic difference of the two sample

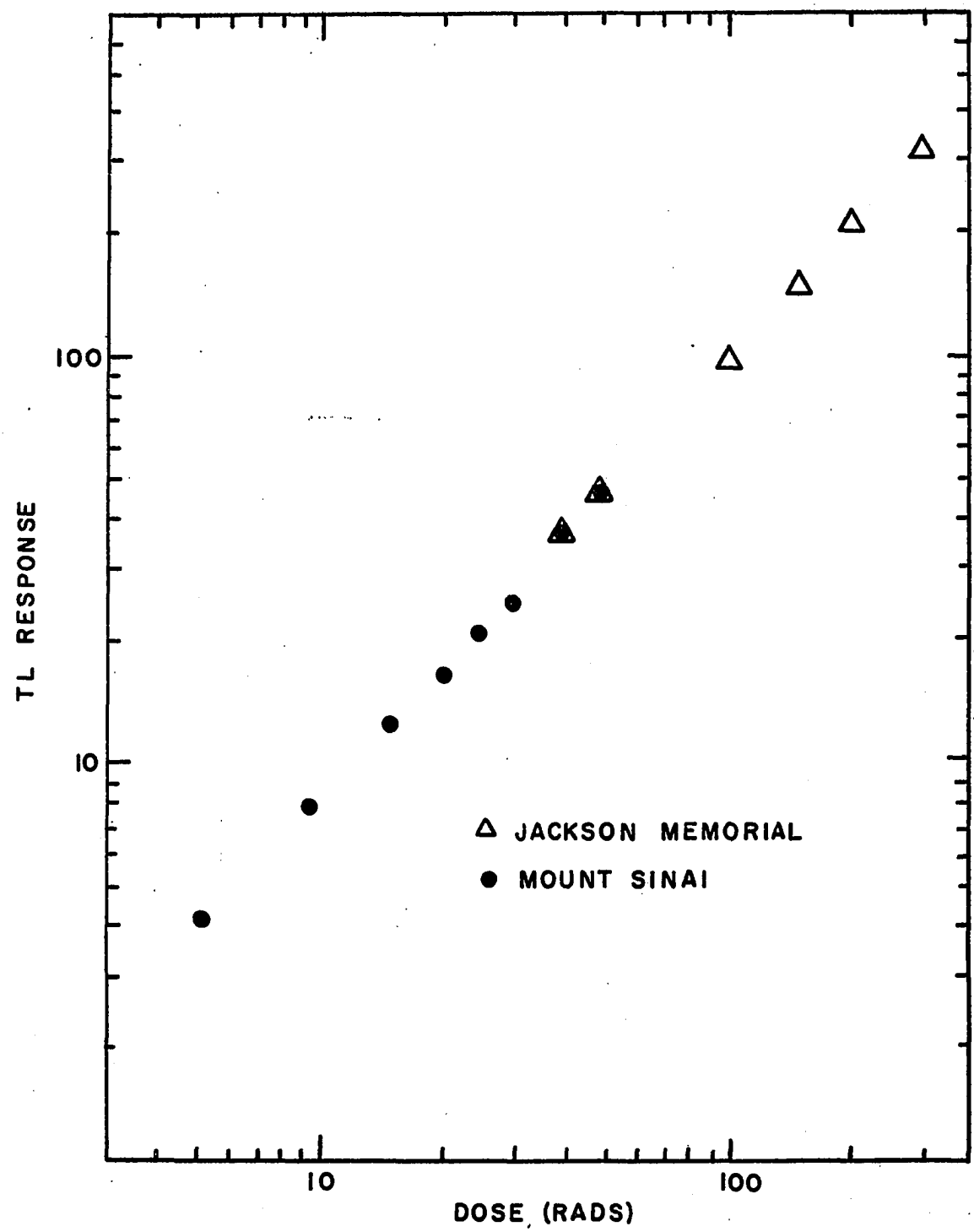

Figure 4. Inter-hospital Calibration Curve: TL Response vs. Dose

readings is zero). The advantage of this method of eliminating NRI-TL variations is noted by Jones and Bjarngard (1968). According to this correspondence, under optimum signal to noise ratio, it is the variations in the background signal and not the absolute magnitude of the background and its components that limit the measurements of lower doses. Thus, taking the difference of subsequential readings for one TL crystal sample corrects for background independently each time and provides a means to reduce the error caused from variations. The advantage of a measured zero is that the stability of the TLD system (dark current and individual TL sample variation) is checked.

CHAPTER III

METHODS AND CALCULATIONS

3.1 Artifacts

Artifact is defined as that effect which results from the imposed geometric conditions. In these studies, artifacts are effects on the dose distribution resulting from the given experimental model. The word model is used to designate the set of assumed spatial, structural, and kinetic conditions for which dose calculations are to be made. Thus, the artifacts to be studied in this dissertation were source edge effects and TLD edge effects of photons in a bounded medium.

The source edge effect study was designed to determine whether or not there was a disturbance of the radiation field by the boundaries of the phantom (i.e. from the model), when the source location was varied with respect to the boundaries.

The TLD edge effect study was planned to analyze the perturbation of the dose distribution occurring from the presence of phantom boundaries.

The phantom material (obtained from James Firdler and Company, Ltd., Mansell Works, Mansell Road, Acton Vale, London W.3, England) is tissue equivalent rubber consisting of polyisoprene ($C_5 H_8$). It is readily machineable and received in slab from (38 cm x 38 cm x 2 cm) for convenient handling. Stacey et al. (1961) have found this vulcanized

rubber compound usable as a tissue equivalent phantom material within the photon energy range 30 to 662 keV. In both the source and the TLD edge effect studies, the phantom was comprised of fourteen slabs of this tissue equivalent rubber stacked vertically to form a rectangular block 38cm x 38cm x 28cm (see Figure 5). The source and TLD's were all inserted into one of the fourteen slabs called the detector slab.

The sources used in this research (Co-57, Sn-113, and Cs-137) were encapsulated in specially designed 1.27cm diameter x 0.635cm deep plastic discs by New England Nuclear Corporation, Boston, Massachusetts (See Figure 2). They were not ideal point sources; however, this fact only introduced a systematic bias of less than 1 per cent standard deviation in a comparison of experimental results made with theoretical point source functions (Ellett, 1969; Meredith et al. 1966). Therefore, the plastic mounted sources were assumed point-approximate.

3.2 Source Edge Effect Study

In order to adequately examine the dose distribution for point-approximate sources in bounded media, the question of any effects on the sources which were finitely near boundaries had to be answered. This study was prompted for later ascertaining that the dose perturbation from a bounded medium was actually caused by the boundary influence on the dose distribution, and not by the boundary effects on both the dose and the source. In addition, this study allowed determination of the precision attainable for the Harshaw LiF-100 extruded rods under the given experimental conditions. Precision is defined

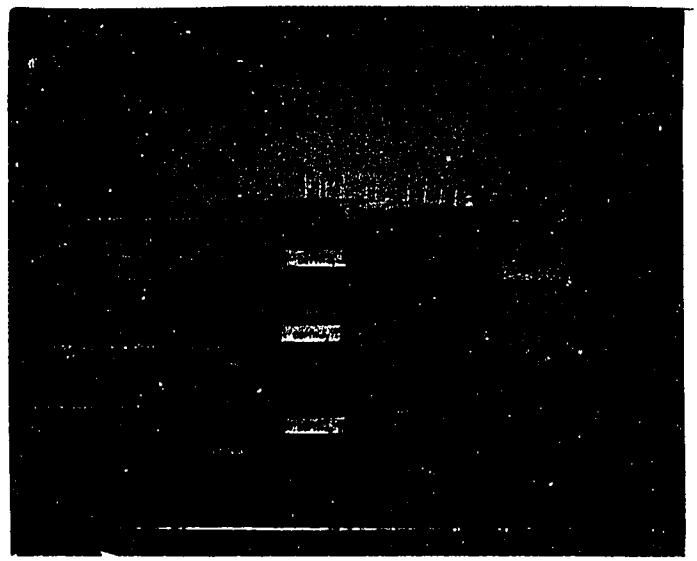

Figure 5. Tissue-Equivalent Rubber Phantom (38 cm x 38 cm x 24 cm).

as a measure of agreement among individual measurements. The results of the precision determined the basis for criteria in the TLD edge effect study.

In designing the detector slab for the source edge effect study, several factors had to be considered. The crucial problem was to include a significant range of source locations with respect to the boundaries, while excluding any boundary effects on the detectors. At the same time the source-to-detector distance had to fulfill two conditions: 1) the dose, accumulated in a reasonable exposure time, was large enough to be measured easily and accurately and 2) the LiF-100 detectors were placed under the same conditions for the precision comparison. The detector slab was centered in the phantom of stacked slabs, so that no vertical-boundary effects would occur, i.e. so that edge effects on the detector slab from the top or bottom of the phantom were negligible.

Figure 6 illustrates the detector slab for the source edge effect. There are three source inserts located on the diagonal of the slab. The perpendicular distances of each of these inserts to both edges are 7cm, 10cm and 14 cm. These distances fall within and without about one mean free path from the edges for each of the three radioactive sources used in the study. The low energy photon (123 keV) of Co-57 has a mean free path (mfp) of about 7cm in the tissue equivalent rubber, the 393 keV photon of Sn-113 has approximately a 9 cm mfp, and the 662 keV photon of Cs-137 has about a 12cm mfp. The TLD inserts were drilled to form an arc 7cm from the source. This distance allowed a sufficient

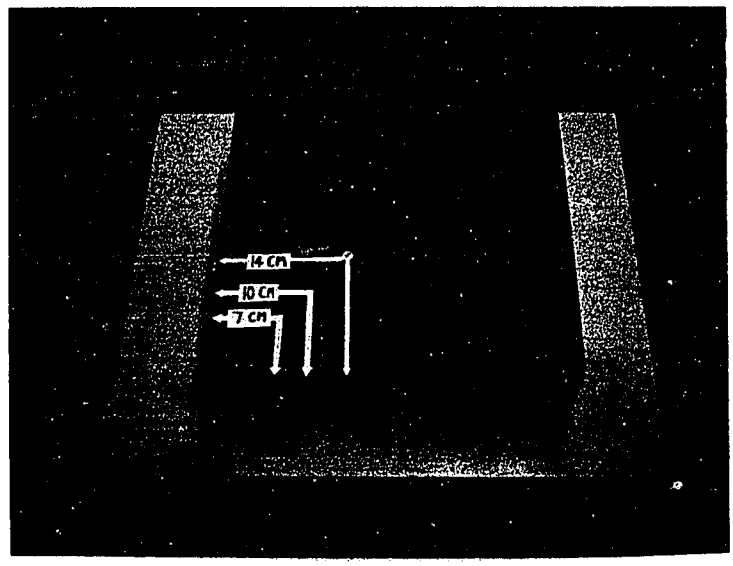

Figure 6. Detector slab for source edge effect study (source-detector distance 7 cm)

dose to be accumulated in a reasonable length of time, and the LiF-100 detectors to be negligibly effected by any boundaries. Since the TLD's were placed in an arc, each one was at the same fixed distance from the source and consequently under equal conditions for comparison of response.

The calculations used to describe the experimental data for the source edge effect study involved the analysis of variance. Variance analysis is a statistical procedure for testing for differences among the means of two or more populations of numbers. This concept was instrumental in making decisions on the possibility of a source edge effect occurring, and on the attainable precision using Harshaw LiF-100 extruded rods.

The precision of TLD measurements (± 3 per cent) is expressed in terms of relative standard deviation. The standard deviation is defined as the positive square root of the variance (Dixon and Massey, 1957). The variance is the sum of the squares of the difference between the individual observations and the mean of all the observations, all divided by the number of observations minus one or,

$$s^2 = \frac{\sum_{i}^{N} (X_i - \bar{X})^2}{N-1} \qquad (14)$$

where:

N = number of observations

X_i = value of observation i

$\bar{X}$ = arithmetic mean value of observations.

The standard deviation is simply the square root of the above variance. The relative standard deviation is defined as the standard deviation devided by the arithmetic mean.

$$\% s = \frac{\sqrt{\frac{\sum_{i}^{N} (Xi-\bar{X})^2}{N-1}}}{\bar{X}} \qquad (15)$$

The precision of the LiF-100 detectors was found as a byproduct in the course of studying the source edge effect.

The process of using samples from a population of numbers to test a hypothesis is called a statistical proof of the hypothesis. The statistical proof of the source edge effect was a comparison of sample means when the universal variance is unknown (the T distribution). The hypothesis is that two populations have the same mean but the universal variance, σ^2, is unknown, i.e. the different source locations have the same mean under equal exposure conditions, and the boundaries do not effect this source data. The decision of accepting or rejecting the hypothesis, i.e. whether the different source locations changed the fluence (a source edge effect), was based on the information obtained by making observations and by assessing an acceptable degree of risk that the decision may be wrong. This chance of risk is called the level of significance, denoted by the Greek letter α. A convention frequently followed is to state the result "significant" if the hypothesis is rejected with $\alpha = 0.05$ and highly "significant" if it is rejected with $\alpha = 0.01$.

The procedure used in the statistical proof was completed in six steps:

1. Hypothesis: Two populations have the same mean. The three different source-detector configurations produce the same mean TL reading, under equal exposure conditions. The mean TL reading of the 7cm source location was compared with the mean TL reading of the 10cm source location and the 14cm source location. Then the mean TL reading of the 10cm source location was compared with the mean of the 14cm source location.

2. The level of significance ($\alpha = .01$) was chosen.

3. For the statistical test use

$$t = \frac{(\bar{X}_1 - \bar{X}_2)}{S_p \sqrt{(1/N_1) + (1/N_2)}} \qquad (16)$$

where S_p is the pooled mean-square estimate of the universal standard deviation σ given by

$$S_p = \left[\frac{(N_1-1)\ S_1^2 + (N_2-1)\ S_2^2}{N_1 + N_2 - 2}\right]^{\frac{1}{2}}$$

where N_1 = number of observations in the first sample,

N_2 = number of observations in the second sample,

S_1 = variance of the first sample

S_2 = variance of the second sample

4. Assuming that both populations have normal distributions with

the same mean and the same universal variance, then this statistic has the $t(N_1 + N_2 - 2)$ distribution to be entered into the T test tables (Dixon and Massey, 1957).

5. The rejection region is

$$t_1 - \frac{1}{2}\alpha(N_1+N_2-2) < t < t_1 - \alpha\,(N_1+N_2-2)$$

6. The computed t is entered into the tables, and the hypothesis is accepted or rejected.

3.3 Dose Edge Effect Study

In the dose (TLD) edge effect study, the perturbation of the dose distribution caused by the presence of boundaries was given experimental interpretation and compared to the theoretical predictions of Ellett (1969).

The TLD edge effect study consisted of taking measurements when the TLD's were located near a phantom edge and comparing them with those situated well within the phantom. The detectors located farthest from the edges were not influenced by boundaries; consequently, they were used as the control values. The detector slab for the study was designed to fulfill these requirements. It was cut to accommodate one plastic mounted source 12cm from both edges and 20 TLD inserts making a quarter circle around the source at 11.5cm away (see Figure 7). This distance is a little more than one mean free path in the rubber phantom for the highest photon energy emitted by the radioactive sources (Co-57, Sn-113, and Cs-137) used in this experiment. The results of the source edge effect study verified that the particular source location

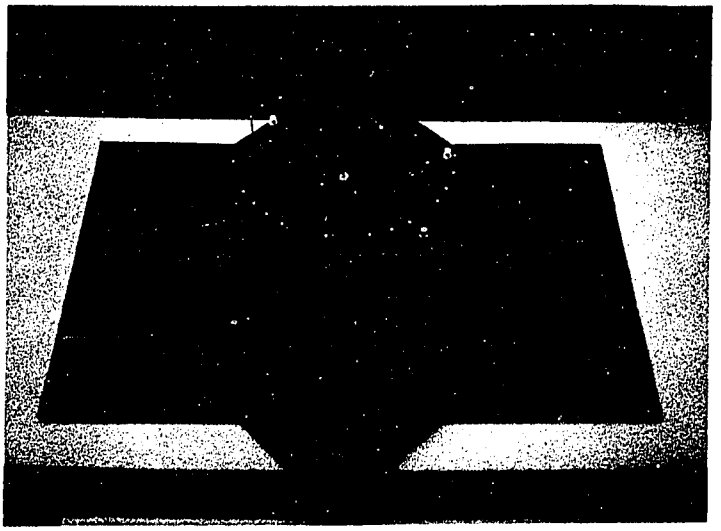

Figure 7. Detector Slab for Edge Effect Study (20 TLD Inserts at 11.5 cm from Sources).

was not an additional variable of any consequence for the edge study. The 12cm source location allowed TLD's to be placed at 0.5cm and 1cm to 19cm in unit integral (cm) steps from the edges of the phantom. This configuration was assumed adequate to describe the perturbed dose distribution in terms of the perpendicular distance from a boundary for the three photon energies (Smith, 1969). No experimental data for edge studies has been published. Greene and Stewart (1965) have published isodose curves for non-uniform phantoms, but did not study the effects which occurred at the boundaries.

As a comparison to minimize error, ratios of TL readings were used, as well as absolute dose measurements. The TLD measurements were defined by numbers 1 through 20 with number 1 being that insert closest to an edge (0.5cm perpendicular from the edge) and increasing numbers clockwise. The ratios were obtained by dividing each TL reading by the average reading of the central six dosimeters (TLD nos. 8-13). The middle-six TL average reading was set equal to 1.0 as the reference (control) value, and all other values were normalized to this reference point. This average is a meaningful control since each of the six TLD positions was sufficiently distant from either edge - at least 13cm - while simultaneously maintained under the same experimental conditions as the remaining positions.

The energy dependence of the perturbed dose distribution was included for the range 123 keV to 662 keV by using Co-57, Sn-113, and Cs-137. A spatial dependence study was included by locating the detector

slab at two different depths in the phantom. The control depth was the same vertically centered depth used in the source edge effect study. The measurements taken at this depth were compared to those taken at the third slab from the top (5cm from the top) of the phantom.

The results were expressed in tabular and graphical form with absolute dose and relative dose versus perpendicular distance from a boundary. However, the parameters used in the variance analysis to estimate the standard deviation of the measured signals from LiF-100 dosimeters followed the statistical analysis convention proposed by Martensson (1969).

The statistical analysis of the standard deviation in this relative dosimetry study used variance analysis and fulfilled the following requirements:

(a) the systematic individual sensitivity differences between the detectors were eliminated;

(b) the systematic changes of sensitivity between repeated experiments were eliminated;

(c) only two consecutive experiments were compared.

The quantities used in this analysis are defined as follows:

Q - is a measure of the total variation within the analyzed values;

Q_A - is a measure of the systematic sensitivity changes of the dosimeters between two consecutive experiments;

Q_B - is a measure of the individual sensitivity differences between the dosimeters;

Q_0 - is a measure of the remaining variations in the values when the systematic effects are eliminated.

Q is that measure of variation which will describe the spatial effect between the two depths used in this study.

Table II illustrates the procedure for performing this variance analysis, to be used in conjunction with the following formulation:

$$Q(\text{total variation}) = \sum_{i}^{n} \sum_{j}^{2} (X_{ij} - \bar{X})^2$$

$$Q_A(\text{systematic sensitivity changes}) = n \sum_{j}^{2} (\bar{X}_{\cdot j} - \bar{X})^2$$

$$Q_B(\text{individual sensitivity changes}) = 2 \sum_{i}^{n} (\bar{X}_{\cdot i} - \bar{X})^2$$

$$Q_0(\text{spatial sensitivity changes}) = Q - Q_A - Q_B$$

Where two consecutive experiments, at the two depths, are performed for n(= 20) number of dosimeters.

The experimental procedures were completed using the above formulated convention. In addition, two more TLD's were taped to the two edges of the detector slab at 12cm from the source for comparison of agreement between each other, and for additional extrapolated values to be included in the dose edge effect study.

Table II. A schematic of the parameters used in the variance analysis to estimate the standard deviation of the measured signals from LiF-100 dosimeters. (X_{ij} is the measured signal from dosimeter i, used in experiment j.)

Dosimeter:	1	2	3	n	
Measurement:					
1	X_{11}	X_{21}	X_{31}	X_{n1}	$\bar{X}_{.1} = \frac{1}{n}\sum_{i=1}^{n} X_{i1}$
2	X_{12}	X_{22}	X_{32}	X_{n2}	$\bar{X}_{.2} = \frac{1}{n}\sum_{i=1}^{n} X_{i2}$
	$\bar{X}_{1.} = \frac{1}{2}\sum_{i=1}^{2} X_{1i}$	$\bar{X}_{2.} = \frac{1}{2}\sum_{i=1}^{2} X_{21}$	$\bar{X}_{3.} = \frac{1}{2}\sum_{i=1}^{2} X_{3i}$	$\bar{X}_{n.} = \frac{1}{2}\sum_{i=1}^{2} X_{ni}$	$\bar{X} = \frac{1}{2n}\sum_{i=1}^{n}\sum_{j=1}^{2} X_{ij}$

CHAPTER IV

EXPERIMENTAL RESULTS

4.1 Source Edge Effect Study

The results of the source edge effect experiment showed that, for the detectors located in the central portion of the phantom and not exposed to edge effects, there is no detectable effect occurring from varying the source location. An effect did not occur within a level of significance of 0.01 for the three energy sources (123 keV, 393 keV, and 662 keV) which were located at 7cm, 10cm, and 14cm perpendicularly from two edges of the tissue equivalent phantom. The attainable precision (agreement among equal dose-exposures) for LiF-100 extruded rods was ±3 per cent relative standard deviation.

Tables III, IV, and V give the data for the source edge effect study. For each source energy, three experimental runs were made; one each with the source location at 7cm, 10cm, and 14cm under equal dose-exposure conditions. The data was expressed in TL units because the precision was more apparent when the readings were in this form. The transition to absolute dose terms tended to mask the slight differences of the TLD readings. The dose-exposures of each source location were kept equal so that no unnecessary error was introduced from having to normalize the measurements. This method also allowed individual measurements to be compared to any one of the other measurements for each source energy.

Table III. Source edge effect study for Cobalt-57

Source Location from Edges of Phantom	TLD Reading	Comments
7cm	0.110 0.107 0.106 0.102 0.105	Relative Standard Deviation = 2.7% t test: p = 0.94
	Average = 0.1060±0.00291	
10cm	0.106 0.104 0.109 0.107 0.102 0.103 0.107	Relative Standard Deviation = 2.4% t test: p = 0.93
	Average = 0.1054±.0025	
14cm	0.104 0.108 0.110 0.105 0.102 0.105	Relative Standard Deviation = 2.6% t test: = 1.00
	Average = 0.1057±0.0027	
	Total Average = 0.1057±0.0027 Overall	Total Relative Standard Deviation = 2.6%

Table IV. Source edge effect study for TIN-113

Source Location from Edges of Phantom	TLD Reading	Comments
7cm	0.121 0.118 0.123 0.124 0.117	Relative Standard Deviation = 2.3% t test: p = 0.71
	Average = 0.1206±0.0028	
10cm	0.124 0.120 0.123 0.125 0.126 0.124 0.122	Relative Standard Deviation = 1.8% t test: p = 0.70
	Average = 0.1234±0.00205	
14cm	0.125 0.119 0.121 0.123 0.119 0.124 0.121	Relative Standard Deviation = 0.20% t test: p = 0.93
	Average = 0.1217±0.0024	
	Total Average = .1220±.0026	Total Relative Standard Deviation = 2.2%

Table V. Source edge effect study for Cesium-137

Source Location from Edges of Phantom	TLD Reading	Comments
7cm	0.403 0.409 0.406 0.421 0.407	Relative Standard Deviation = 0.8% t test: p = 0.83
	Average = 0.4092±0.0031	
10cm	0.405 0.409 0.417 0.416 0.413 0.412 0.415	Relative Standard Deviation 0.4% t test: p = 0.73
	Average = .4124±0.0016	
14cm	0.417 0.412 0.403 0.411 0.403 0.411 0.411	Relative Standard Deviation = 1.0% t test: p = 0.88
	Average = 0.4097±0.004	
	Total Average = 0.4105±0.00525	Total Relative Standard Deviation = 1.3%

From all measurements taken for each source location, an average reading and a relative standard deviation was computed by the methods described in Chapter III, Section 3.2. The statistical proof (the T distribution of Dixon and Massey, 1957) was performed between pairs of source locations, and the significance $\alpha = .01$ was valid in all cases. In addition, an average reading and a relative standard deviation were determined for all measurements taken for each energy. These results agreed well with those taken for the individual source locations. Using this overall mean and relative standard deviation, the t test of significance described by Chase and Rabinowitz (1967) was also performed for each source location data. This t test was designed to determine the probability that the difference between two observed measurements is due to technique, or that the observed difference may be attributed to statistical fluctuations. The t test is a modified version of the Dixon and Massey (1957) T distribution.

In this test, the samples were statistical duplicates, i.e. the mean TL reading, at any one source location for a particular energy, was considered to possess the same statistical properties as the overall mean. These circumstances were accomplished by maintaining equal dose-exposure conditions. Under these conditions, the sample variance of difference S_D^2 is equal to the sum of the variances of each sample observation,

$$S_D^2 = S_1^2 + S_2^2 \qquad (17)$$

where S_1^2 = variance of all measurements for the particular energy source

S_2^2 = variance of measurements at one source location

and the number of standard deviations in the difference is defined by:

$$t = \frac{\text{difference of the means}}{\text{sample standard deviation of difference}}$$

$$t = \frac{\bar{X}_1 - \bar{X}_2}{S_D} \tag{18}$$

The value of t is entered into the cumulative normal frequency distribution table, and the probability, p, that the difference of means is due to technique is obtained. The results were good considering the assumption depended on ideal systematic biases, which are not completely controllable (see Tables III, IV and V). Nevertheless, having tested the results using the two methods with good results, it was shown that, under the experimental conditions used here, there is no detectable source edge effect occurring in the bounded medium.

Recent computer studies have confirmed this prediction but expressed their results in terms of absorbed fraction (see Chapter I, Section 1.4). Ellett et al. (1964) stated that for elliptical cylinders "the linearly increased escape of radiation as a source is moved towards the surface is largely compensated by increased absorption in the opposite direction". Another interpretation of this statement would be that the radiation field remains largely unchanged when

the source is moved towards a boundary. Fisher and Snyder (1968) at Oak Ridge National Laboratory, ORNL, found similar results in their computer calculations applying the dose reciprocity theorem for internal sources within their 70kg homogeneous anthropomorphic phantom. Therefore, both computer calculations and experimental verification justified the use of the detector slab geometry for the dose edge effect study to be discussed next.

4.2 Dose Edge Effect Study

The results of the dose edge effect study in Figures 8, 9 and 10 show that the general shape and magnitude of the experimental curves agree reasonably well with the computer predictions of Ellett (1969). The depth values (perpendicular distances from nearest boundary for no edge effect obtained experimentally did not agree so well with the depth value for the computer data. This disagreement could be due to the geometry differences between the computer and experimental studies. In Figures 8, 9 and 10, the experimental dose distribution from the central detector slab is compared in absolute and relative units with the computer results for Co-57, Sn-113 and Cs-137 respectively. The bars at the experimental points represent the range of one standard deviation for the four experimental runs.

Relative to the dose at the same distance from the source in an unbounded medium, the absorbed dose at a non-reflecting boundary (such as the rubber-air interface of this study) is reduced for two reasons; some energy in the form of kinetic electrons leaves the phantom and

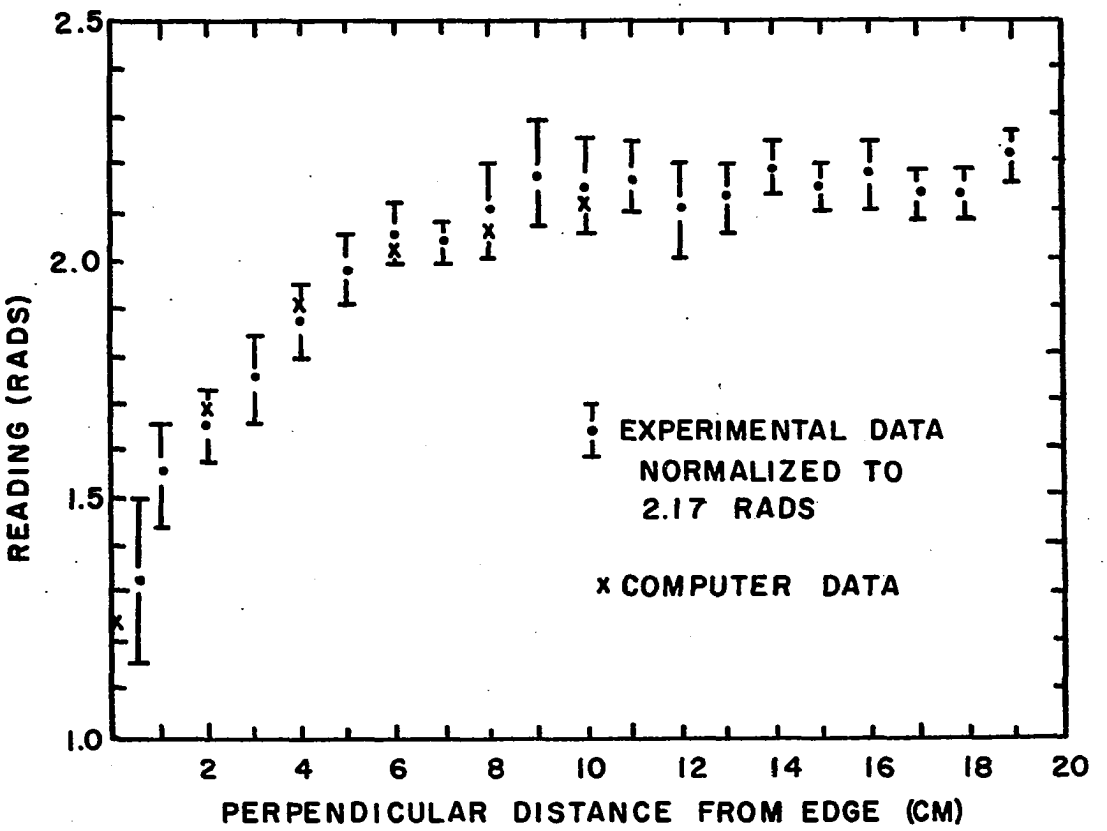

Figure 8. Co-57 Edge Effect Plot

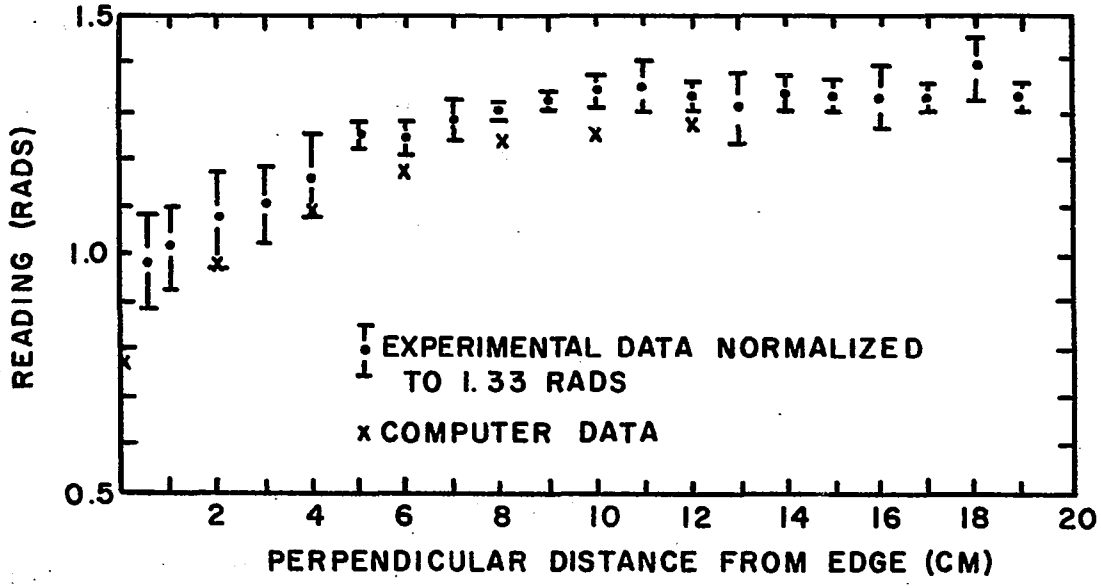

Figure 9. Sn-113 Edge Effect Plot

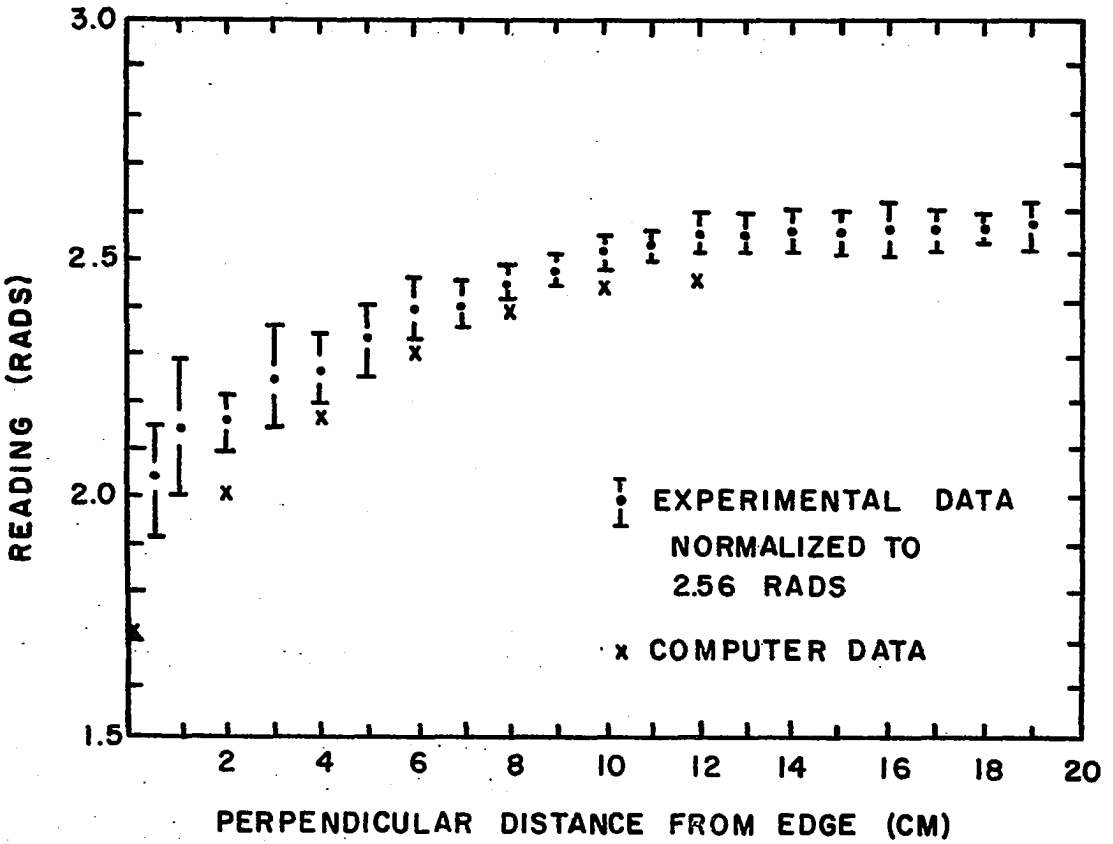

Figure 10. Cs-137 Edge Effect Plot

there are fewer scattered photons. The amount that the absorbed dose is decreased at locations near the boundary is primarily a function of the source energy, and the distance from the boundary. Perturbations in the dose distribution caused by a non-reflecting boundary are rather localized; "the dose is greater than 95 per cent of its value in an infinite medium at all locations more than one mean free path from a boundary" (Ellett, 1969). Therefore, in phantoms having dimensions greater than 2-3 mean free paths only the perpendicular distance to the closest boundary is important.

Tables VI, VII and VIII (Co-57, Sn-113, and Cs-137, respectively) give the absorbed dose values in the phantom relative to the average dose for the middle-six TLD's (nos. 8-13). These experimental ratios are compared to relative values calculated by Ellett (1969). The ratios from Ellett are specific absorbed fractions, Φ, in a bounded medium relative to Φ at the same distance from the source in an infinite medium. From Chapter I, Section 1.4, it is obvious that these same ratios are applicable as dose ratios. The slight differences of the experimental relative dose from the computer relative dose may be attributed to the fact that the experimental ratio depended on the "unbounded" dose value whereas the computer ratio had an approximation of an "infinite" dose value. In addition, the computer ratios were calculated for slightly different source energies and tissue material. Nevertheless, the differences are not large enough to warrant the use of another reference; in fact, the experimental absolute dose distribution of Figures 8, 9, and 10 were favorably compared to these computer ratios.

Table VI. Edge effect ratios for Cobalt-57 (6.3cm mfp).

TLD No.	Perpendicular (cm)	Experimental Dose Ratio	TLD No.	Perpendicular (cm)	Experimental Dose Ratio	Computer Ratio[2] (140 keV) 6.6cm mfp
1	0.5	0.6129	11	19	1.023	-
2	1	0.7142	12	18	0.9815	-
3	3	0.8087	13	16	1.0046	-
4	5	0.9124	14	14	1.0115	-
5	7	0.9354	15	12	0.9723	-
6	9	1.0046	16	10	0.9953	0.98
7	11	1.0000	17	8	0.9723	0.95
8	13	0.9815	18	6	0.9493	0.93
9	15	0.9907	19	4	0.8617	0.88
10	17	0.9838	20	2	0.7603	0.78

[2]Ellett (1969)

Table VII. Edge effect ratios for Tin-113 (9.3cm mfp).

TLD No.	Perpendicular (cm)	Experimental Dose Ratio	TLD No.	Perpendicular (cm)	Experimental Dose Ratio	Computer Ratio[3] (364keV) 9.1cm mfp
1	0.5	0.7368	11	19	0.9962	-
2	1	0.7593	12	18	1.0451	-
3	3	0.8308	13	16	0.9962	-
4	5	0.9398	14	14	1.0037	-
5	7	0.9548	15	12	0.9962	0.96
6	9	0.9924	16	10	1.0075	0.94
7	11	1.0112	17	8	0.9699	0.92
8	13	0.9812	18	6	0.9323	0.89
9	15	1.0000	19	4	0.8721	0.82
10	17	0.9962	20	2	0.8045	0.73

[3]Ellett (1969)

Table VIII. Edge effect ratios for Cesium-137 (11.7cm mfp)

TLD No.	Perpendicular (cm)	Experimental Dose Ratio	TLD No.	Perpendicular (cm)	Experimental Dose Ratio	Computer Ratio[4] (662 keV) 11.7cm mfp
1	0.5	0.7968	11	19	1.0039	-
2	1	0.8398	12	18	1.0019	-
3	3	0.8789	13	16	1.0000	-
4	5	0.9101	14	14	1.0019	-
5	7	0.9394	15	12	0.9980	0.97
6	9	0.9687	16	10	0.9804	0.95
7	11	0.9843	17	8	0.9570	0.93
8	13	0.9980	18	6	0.9335	0.90
9	15	0.9980	19	4	0.8847	0.85
10	17	0.9980	20	2	0.8437	0.79

[4]Ellett (1969)

Since the experimental data did agree reasonably well with the computer calculations, the conclusions made by Ellett (1969) may well apply to this study. However, the real fact shown in Figures 8, 9, and 10, besides the true dose distribution, is that for the low energy Co-57 the edge effect is more pronounced than for the other two higher energies. With the aid of these results, the absorbed dose at a point in a bounded medium can be determined by multiplying the appropriate ratio times the dose calculated for the "infinite" medium. The validity of the theoretical assumption for an unbounded geometry (i.e., configurations of medium, source, and detector such that leakage of radiation across the boundaries of the medium has no influence on the absorbed dose received by the detector) is demonstrated for each energy in these figures. The conditions for the media to be, in effect, unbounded are often assumed satisfied if both the source and the detector are located at least a phantom mean free path from the nearest boundary.

The results of the edge effect study showed this assumption to be a reasonable one for the experimental model used. In Table IX, the depths where the edge effect became apparent are given in absolute (cm) and mean free path (λ) units for the three energy sources. These distances were obtained by two methods (see Appendix A). First, the T distribution (Dixon and Massey, 1957) was performed with a level of significance of 0.01. The first data point that did not meet the criteria for the T distribution test was designated as the initial depth (statistical) where the edge effect became apparent; the other points

Table IX. Depths in phantom for no edge effect.

	Co-57	Sn-113	Cs-137
Graphical:	9.0 cm	9.5 cm	12.0 cm
	1.43mfp	1.02mfp	1.02mfp
Statistical:	9.0 cm	9.0 cm	12.0 cm
	1.43mfp	0.97mfp	1.02mfp
Computer:	12.0 cm	15.0 cm	17.0 cm
	1.91mfp	1.61mfp	1.45mfp
Mean Free Path (mfp):	6.3 cm	9.3 cm	11.7 cm

closer to the boundary also did not meet the criteria. Second, the first data point starting from the boundary which had at least the same magnitude as the normalized dose value was chosen as the initial depth (experimental and computer) for the non-existence of the edge effect. The statistical and graphical depths were in good agreement; the computer distance was larger compared to the other two. The data presented in Table IX shows that with increasing source energy the depths also increased.

The spatial dependence, which was studied by locating the dose edge effect detector slab at two different heights, is illustrated in Figures 11, 12 and 13 for Co-57, Sn-113, and Cs-137, respectively. In Table X, the variances (defined in Chapter III, Section 3.3) are listed for the three sources. The initial values of variances are the calculations for the two heights as first determined from the measurements; the corrected variances are computations of the measurements which have been corrected for an edge effect. After dividing the measurements for the (highest) slab obtained in the slab located 5cm from surface, by the appropriate boundary correction ratio (for 5cm from nearest boundary at the given source energy) the magnitudes of the relative standard deviations became very small. Also from Table X, the listed differences of the two variances demonstrates that the total variations Q and the systematic sensitivity changes Q_A are the real functional variables which were corrected; the individual sensitivity changes Q_B and the remainder Q_0 were not significantly effected. Therefore, the spatial

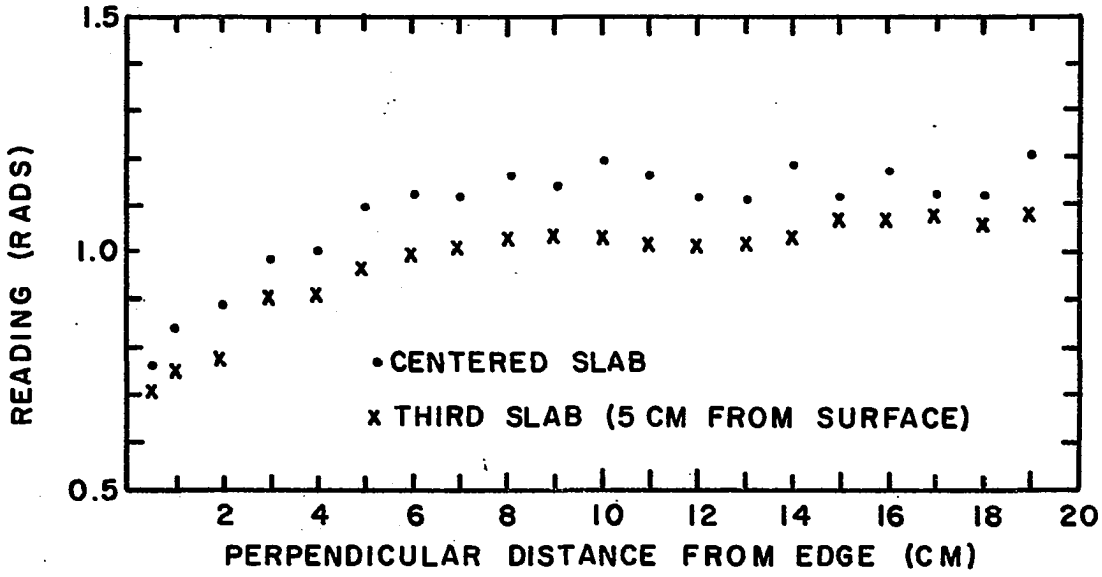

Figure 11. Co-57 Spatial Experimental Plot

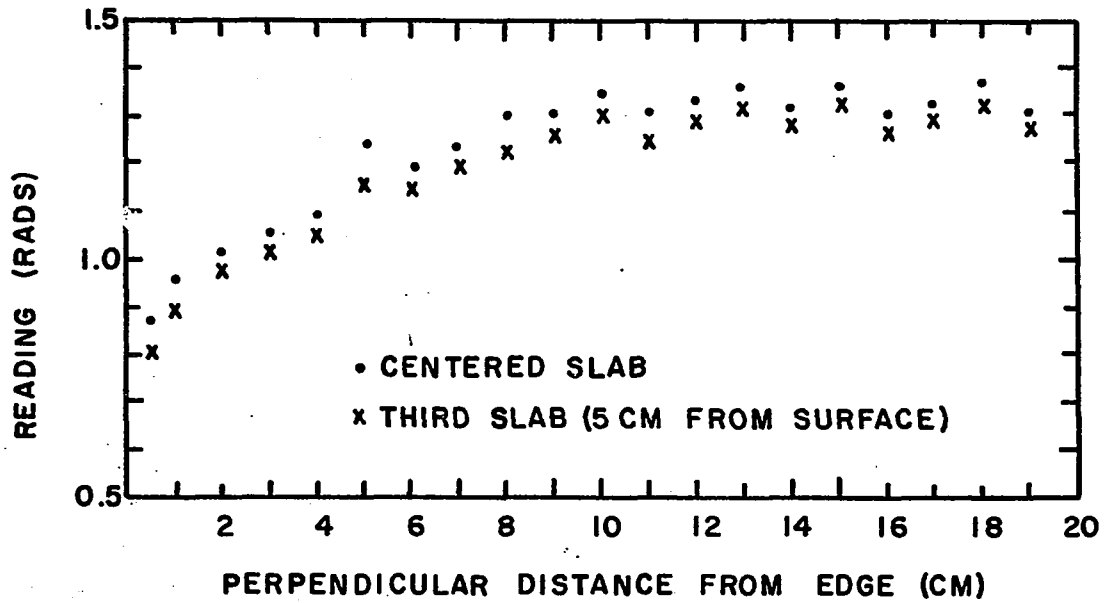

Figure 12. Sn-113 Spatial Experimental Plot

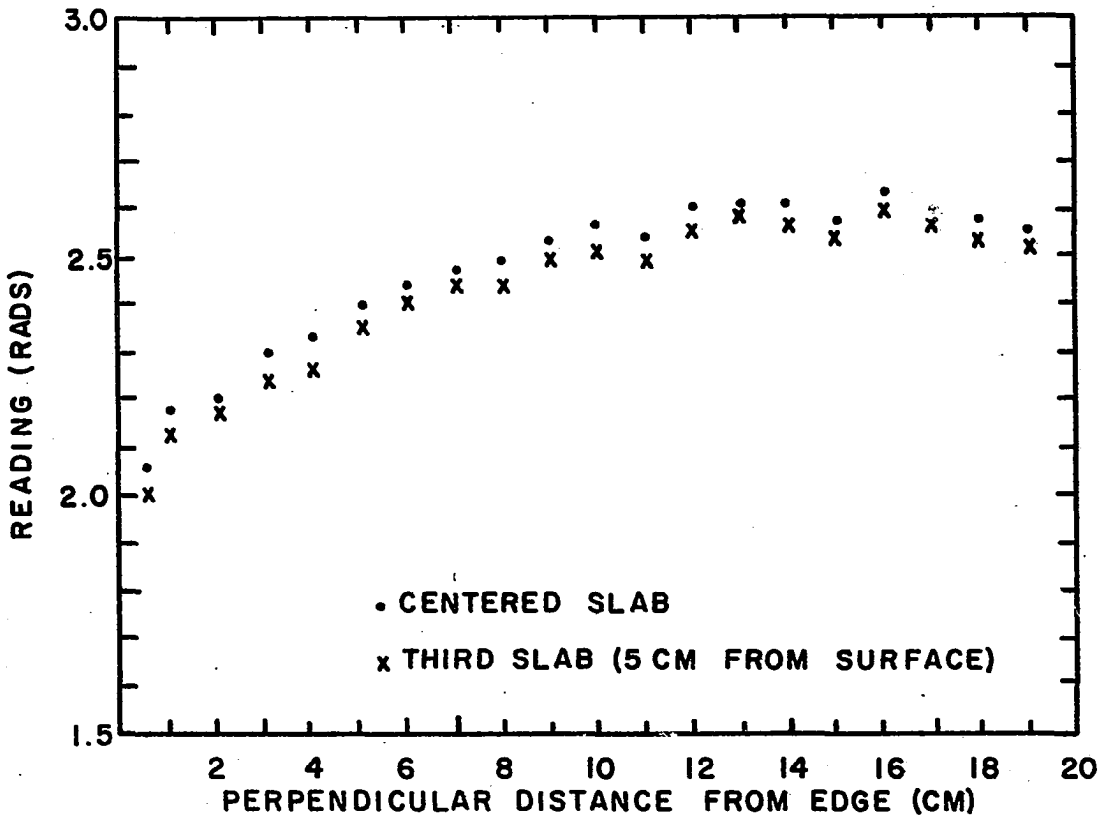

Figure 13. Cs-137 Spatial Experimental Plot

Table X. Variance analysis for spatial study.

Initial Values		Corrected Values	Difference
Cobalt-57			
$Q = 0.0124$	Total Variation	$Q = 0.0105$	$= +0.0019$
$Q_A = 0.0029$	Systematic Sensitivity Change	$Q_A = 0.00002$	$= +0.0029$
$Q_B = 0.0091$	Individual Sensitivity Change	$Q_B = 0.0101$	$= -0.0010$
$Q_0 = 0.0004$	Remainder	$Q_0 = 0.0003$	$= +0.0001$
% S.D. = 9.0		% S.D. = 7.8	
Tin-113			
Initial Values		Corrected Values	Difference
$Q = 0.0113$	Total Variation	$Q = 0.0096$	$= +0.0017$
$Q_A = 0.0009$	Systematic Sensitivity Change	$Q_A = 0.000002$	$= +0.0009$
$Q_B = 0.0089$	Individual Sensitivity Change	$Q_B = 0.0094$	$= -0.0005$
$Q_0 = 0.0015$	Remainder	$Q_0 = 0.0002$	$= +0.0013$
% S.D. = 11.4		% S.D. = 10.1	
Cesium-137			
Initial Values		Corrected Values	Difference
$Q = 0.0245$	Total Variation	$Q = 0.0166$	$= +0.0079$
$Q_A = 0.0095$	Systematic Sensitivity Change	$Q_A = 0.00003$	$= +0.0095$
$Q_B = 0.0146$	Individual Sensitivity Change	$Q_B = 0.0159$	$= -0.0013$
$Q_0 = 0.0004$	Remainder	$Q_0 = 0.0007$	$= -0.0003$
% S.D. = 22.8		% S.D. = 17.8	

dependence of the dose edge effect study for the two depths was found to merely be another boundary effect acting equally on all detector points. That is, the boundary effects occurring within one plane of a detector slab is not changed by imposing a "surface" edge effect.

CHAPTER V

DISCUSSION OF RESULTS

5.1 Summary

The dose distribution in a bounded absorber was investigated as a function of source location and of the perpendicular distance between the location of interest and a boundary, for three primary photon energies (123 keV, 393 keV, and 662 keV). In evaluating the experimental perturbation of the dose distribution in a bounded medium, Harshaw LiF-100 extruded rods were exposed to three monoenergetic point-isotropic gamma sources (Co-57, Sn-113, and Cs-137), in two independent experimental models. It was shown that there exists no detectable effect on the thermoluminescent dose readings when a constant source-to-detector geometry was varied with respect to the boundaries of the experimental phantom. The modification of the experimental dose distribution due to the effects of the boundaries was shown graphically as a function of perpendicular distance from the nearest boundary. In addition the critical region where edge effects occurred was determined. The edge effect on one plane of the detector slab was found to be independent of whether or not the slab was 5cm from the top of the phantom or centrally located in the phantom. The methodology of thermoluminescent dosimetry and of internal dose calculations was also discussed.

The fact that there was no source edge effect verified the computer predictions of Ellett (1969) and Fischer and Snyder (1968); and the experimental dose distribution in the finite phantom also agreed well with

the predictions for the effect on photons in bounded media (Ellett, 1969). The experimental phantom, sources, and detectors were good approximations for point-isotropic, tissue-equivalent, homogeneous models. Variance analysis was maintained for all measurements, and expedited the determination of conclusions.

The results of this dissertation can be used to compute the absorbed dose in clinical dosimetry with increased ease and accuracy.

5.2 Conclusions

As a result of the use of thermoluminescent dosimeters to study the edge effect of photons in a tissue-equivalent rubber phantom, the following conclusions are drawn:

1. The different locations of three monoenergetic point-isotropic gamma sources (123 keV, 393 keV, and 662 keV) with respect to the boundaries of this phantom did not affect the TLD detectors located in the central portion of the phantom, within a level of significance of 0.01.

2. There exists a definite edge effect on the dose distribution near the boundaries for the three sources studied.

3. For the 123 keV photons of Co-57, no edge effect occurred at a depth of 9 cm (1.43 mean free paths) or greater in the phantom.

4. For the 393 keV photons of Sn-113, no edge effect occurred at the depth of 9.5 cm (1.02 mean free paths) or greater in the phantom.

5. For the 626 keV photons of Cs-137, no edge effect occurred at a depth of 12 cm (1.02 mean free paths) or greater in the phantom.

6. Maximum measured edge effect of approximately 39 per cent occurred at the closest distance to a boundary (0.5 cm).

7. The experimental edge effects agreed reasonably well with the computer studies.

8. The edge effect in the plane of the detector was unaffected by the edge effect in the perpendicular plane.

9. Thermoluminescent dosimeters are effective measuring devices for point dose determinations.

5.3 Projected Studies

In the course of this research, new areas of interest became apparent. The need for further research on these subjects has been started, and is only mentioned here as proposals for those seeking dissertation topics and for others as points of interest.

The formulation of MIRD Committee (MIRD, 1968) offers two topics that need experimental analysis. First, the determination of absorbed fraction ϕ, which is simply the fraction of the emitted photon energy that is absorbed in the region of interest, is commensurate with the techniques of thermoluminescent dosimetry; computer studies of ϕ are presently being experimentally verified. Second, the MIRD internal dose equation has the property such that, for materials of different mass density and composition, the tabular entry for the MIRD ϕ values can be appropriately corrected by a density-transformation rule. Experimentally, this property for different materials (eg. lung and tissue) needs verification.

Finally, the use of thermoluminescent dosimetry offers many additional opportunities for research. The reciprocity theorem (Fisher and Synder, 1968) is one such topic which has been experimentally studied by the author of this dissertation. Other available research studies using thermoluminescent dosimetry need only the creative thinker.

REFERENCES

Attix, F.H. (ed): Luminescence Dosimetry, Proc. Internatl. Conference on Luminescence Dosimetry, Stanford University, Stanford, California, June 21-23, 1965. Published as CONF-650637, Clearinghouse for Federal Scientific and Technical Information, U.S. Department of Commerce, Springfield, Virginia, April 1967.

Attix, F.H.: "Isotopic Effect in Lithium Fluoride Thermoluminescent Dosimeters", Phys. Med. Biol. 14(1):147-148, 1969.

Barnard, G.P.: "Dose-Exposure Conversion Factors for Megavoltage X-Ray Dosimetry", Phys. Med. Biol. 9(3):321-332, 1964.

Braunlich P., Schafer D., and Scharmann A.: "A Simple Model for Thermoluminescence and Thermally Stimulated Conductivity of Inorganic Photoconducting Phosphors and Experiments Pertaining to Infrared-Stimulated Luminescence" CONF-650637, p. 57-73, April 1967.

Brownell, G., W. Ellett and A. Reddy: Absorbed Fractions for Photon Dosimetry. J. Nucl. Med. Suppl. 1, p. 27, 1968.

Burch, W.M.: "Two Level Isothermal Read-out for High Precision Thermoluminescence Dosimetry with LiF," Phys. Med. Biol. 13(14): pp. 627-634, 1968.

Cameron, J.R., et al., Science, Volume 134, pp. 333-334, August 1961.

Cameron, J.R., et al.: "Notes on Thermoluminescent Dosimetry", unpublished data (Madison Workshop Notes), University of Wisconsin, January 1967.

Cameron, J.R., D.W. Zimmerman, and R.W. Bland: "Thermoluminescence Vs. Roentgens in Lithium Fluoride: A Proposed Mathematical Model", CONF-650637, pp. 47-56, April 1967.

Cameron, J.R., N. Suntharalingam, and G.N. Kenney: Thermoluminescent Dosimetry, Madison, The University of Wisconsin Press, 1968.

Carlsson, C.A.: "Thermoluminescence of LiF: Dependence of Thermal History", Phys. Med. Biol. 14(1) pp. 107-118, 1969.

Chase, G.D., and J.L. Rabinowitz: Principles of Radioisotope Methodology Minneapolis, Burgess Publishing Company, 1967.

Clichet J. and H. Joffre: "Applications of Thermoluminescence Dosimetry in Health Physics", CONF-650637, pp. 349-358, April 1967.

Private Communication with F. Morgan Cox, Certified Health Physicist, Harshaw Chemical Company, Crystal-Solid State Department, Cleveland, Ohio.

Dillman, L.T.: "Radionuclide Decay Schemes and Nuclear Parameters for Use in Radiation-Dose Estimation", Journal of Nuclear Medicine, Supplement Number 2, Pamphlet 4, March 1969.

Dixon, W.J. and F.J. Massey: Introduction to Statistical Analysis, New York, McGraw-Hill Book Co., (second Ed.), 1957.

Ellett, W.H., A. Callahan, and G. Brownell, "Gamma-ray Dosimetry of Internal Emitters" Monte Carlo Calculations of Absorbed Dose from Point Sources. Brit. J. Radiol. 37, 45, 1964.

Ellett, W.H.: "Application of Gamma-Ray Diffusion Theory to Radiation Dosimetry", Research Report #69-1, Neuro-research Foundation Incorporated, March 1969.

Endres, G.W.R.: "Dosimetry Technology Studies", BN WL-339, pp. 1-10, 1965.

Fano, U., L. Spencer, and M. Berger: "Penetration and Diffusion of X-rays", Handbuch der Physik, 38, 2, ed. by S. Flügge, Springer Verlag, Berlin, 1959.

Fisher, H., and W. Snyder: Proceedings of First International Congress of International Radiation Protection Association. Pergamon Press, Oxford, 1968.

Greene, D., and J.G. Stewart: "Isodose Curves in Non-Uniform Phantoms", Brit. J. Radiology 38: pp. 378-385, 1965.

Hall, R.M.: "Development and Applications of Thermoluminescent Dosimeters", DPMS-66-29, June 1966.

Harris, A.M., and J.H. Jackson: "Pre-Irradiation Annealing of TLD Lithium Fluoride", Health Physics 15: pp. 457-461, 1968.

Harshaw Chemical Company, Crystal-Solid State Department: Model 2000 TLD System Operating Instructions, Cleveland, Ohio, 1967.

Hine, G.J. and G. Brownell, eds.: Radiation Dosimetry, New York, Academic Press, pp. 718-781, 1964.

Hospital Physicists' Association: "A Code of Practice for the Dosimetry of 2 to 35 MV X-ray and Cesium-137 and Cobalt-60 Gamma-ray Beams", Phys. Med. Boil. 14(1):1-8, 1969.

I.C.R.U.: Report of the International Commission on Radiological Units and Measurements. In N.B.S. Handbook 62, Superintendent of Documents, U.S.G.P.O., Washington, D. C., 1956.

I.C.R.U.: Recommendations of the International Commission on Radiological Units. Report 10a, Radiation Quantities and Units. Report 10b, Physical Aspects of Irradiation in N.B.S. Handbook 85, Superintendent of Documents, U.S.G.P.O., Washington, D. C., 1962.

International Commission on Radiological Protection: Report of Committee II on Permissible Dose for Internal Radiation, London, Pergamon Press, 1959.

Johns, H.E.: The Physics of Radiology, Springfield, Illinois, Charles C. Thomas, Second Edition, 1964.

Jones, D.E., J.R. Gaskell, A.K. Bart, and Blocks: USAEC Report UCRL-12151, Lawrence Radiation Laboratory, University of California, October 14, 1964.

Jones, D.E., K. Petrock, and D. Denham: "Thermoluminescent Materials for Personnel Monitoring in Gloved Box Operations", TID-4500, UV-41, pp. 33-35, 1966.

Jones, D. and B.E. Bjarngard: "The Limitations in Low Radiation Dose Measurements Using Thermoluminscence", Phys. Med. Biol. 13(3) pp. 461-466, 1968.

Karzmark, C.J., J. White, and J.F. Fowlet: "Lithium Fluoride Thermoluminescent Dosimeter Powder", Phys. Med. Biol. Volume 9, No. 3, p. 273, July 1964.

Karzmark, C.J. et al.: "Problems of Reader Design and Measurement Error in Lithium Fluoride Thermoluminescent Dosimetry", Int. J. Appl. Rad. and Isotopes 17: pp. 161-173, 1966.

Lin, F.M., and J.R. Cameron: "A Bibliography of Thermoluminescent Dosimetry", Health Physics 14: pp. 495-514.

Loevinger, R, and M. Berman: A Scheme for Absorbed-dose Calculations for Biologically-distributed Radionuclides. J. Nucl. Med. Suppl. 1, p. 7, 1968.

Marinelli, L., E. Quimby, and G. Hine: "Dosage Determination with Radioactive Isotopes. II. Practical Considerations in Therapy and Protection". Amer. J. Roentganol. Rad. Ther., 59, p. 260, 1948.

Martensson, B.K.S.: "Thermoluminescence of LiF: A Statistical Analysis of the Influence of Pre-annealing on the Precision of Measurement", Phys. Med. Biol. 14(1): pp. 119-130, 1969.

Mayneord, W.: "Energy Absorption". Brit. J. Radiol. 13, p. 235, 1940.

Mayneord, W.: "Energy Absorption". III. The Mathematical Theory of Integral Dose and its Applications in Practice". Brit. J. Radiol. 17, p. 359, I944.

Mayneord, W. and J. Clarkson: "Energy Absorption. II. Integral Dose when the Whole Body is Irradiated". Brit. J. Radiol. I7, p. 151, 1944.

Mayneord, W.: "Energy Absorption. IV. The Mathematical Theory of Integral Dose in Radium Theory". Brit. J. Radiol. 18, p. 12, 1945.

Meredith, W., D. Green and K. Kawashima: "The Attenuation and Scattering in a Phantom of Gamma-rays from Some Radionuclides used in Mould and Interstitial Gamma-ray Therapy". Brit. J. Radiol. 39, p. 280, 1966.

MIRD Committee, Journal of Nuclear Medicine, Supplement No. 1, Pamphlets 1-3, Feb. 1968.

Palmer, R.C.: "A Prototype LiF Radiation Dosimeter for Personnel Monitoring", Int. J. Appl. Radiat. Isotopes, Volume 17, p. 413, 1966.

Randall, J.T., and M.H.F. Wilkins: "Phosphorescence and Electron Traps, I. The Study of Trap Distributions", Proc. Royal Soc. (London). Series A 184: p. 365, 1945.

Smith, E.M. (ScD): private communication associate professor, University of Miami, Miami, Florida.

Stacey, A. J., A. R. Bevan and C. W. Dickens: "A New Phantom Material Employing Depolymerized Natural Rubber", Brit. J. Radiology 34, p. 404, August 1961.

Suntharalingam, N., D.W. Zimmerman, and G.N. Kennn: "Personnel Dosimetry with Single Crystals of Lithium Fluoride", Luminescence Dosimetry (F. H. Attix, editor) pp. 217-226, April 1967.

Suntharalingam, N., et al.: "Fading Characteristics of Thermoluminescent Lithium Fluoride", Phys. Med. and Biol., Volume 13, p. 97-104, 1968.

Tochilin, E., and N. Goldstein: "Dose Rate and Spectral Measurements from Pulsed X-Ray Generators", DASA 1703, USNRDL-TR-939, December 1965.

Appendix A

Table XI. T Distribution Test for Cs-137.

Depth (cm)	mean	Standard Deviation ($x10^{-2}$)	t
½	2.04	11.6	24.41
1	2.15	13.6	16.53
2	2.16	6.5	33.33
3	2.25	11.1	15.12
4	2.265	7.4	22.22
5	2.33	7.6	16.43
6	2.39	5.5	17.00
7	2.405	4.1	19.84
8	2.45	2.0	29.10
9	2.48	2.5	5.49
10	2.51	2.5	10.89
11	2.52	2.6	8.23
→ 12	2.555	3.2	0.86
13	2.55	3.3	1.62
14	2.575	2.6	2.46
15	2.55	3.7	1.45
16	2.56	5.9	0.28
17	2.555	3.2	0.86
18	2.565	2.2	0.40
19	2.57	4.5	1.22

Overall mean = 2.5629 ± 0.037

$t_{.01}(26\text{d.f.}) = 2.479$

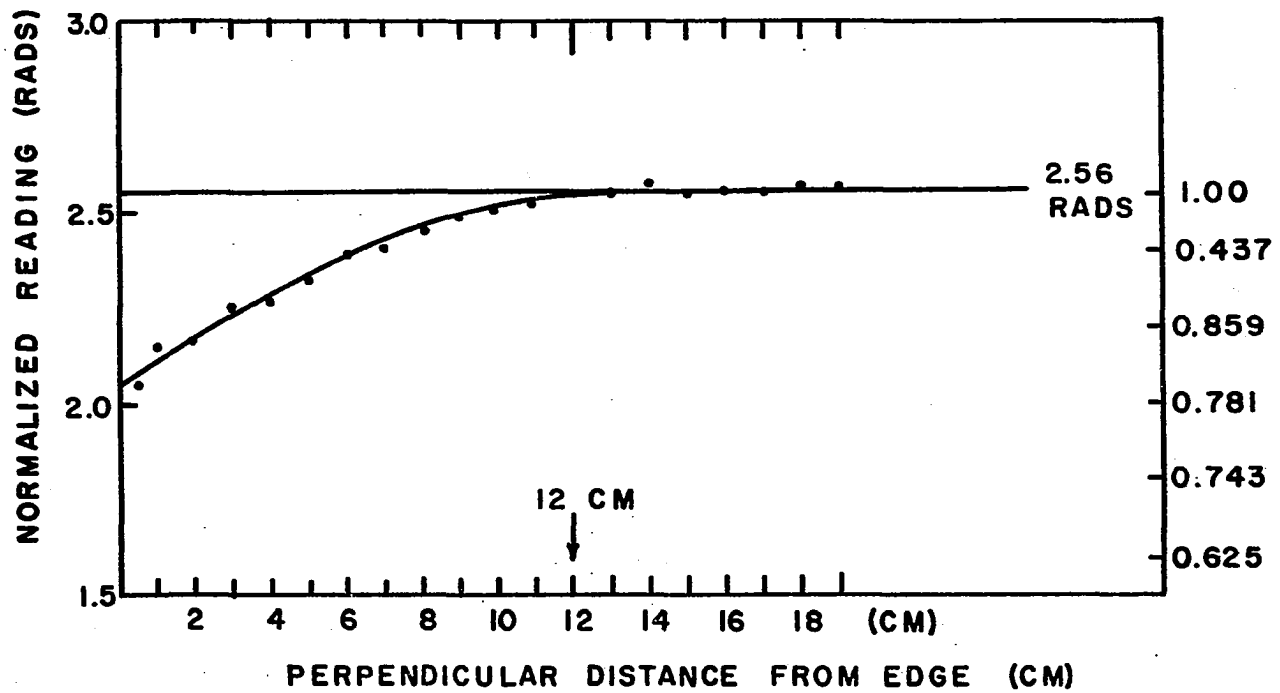

Figure 14. Experimental Edge Effect Graph for Cs-137

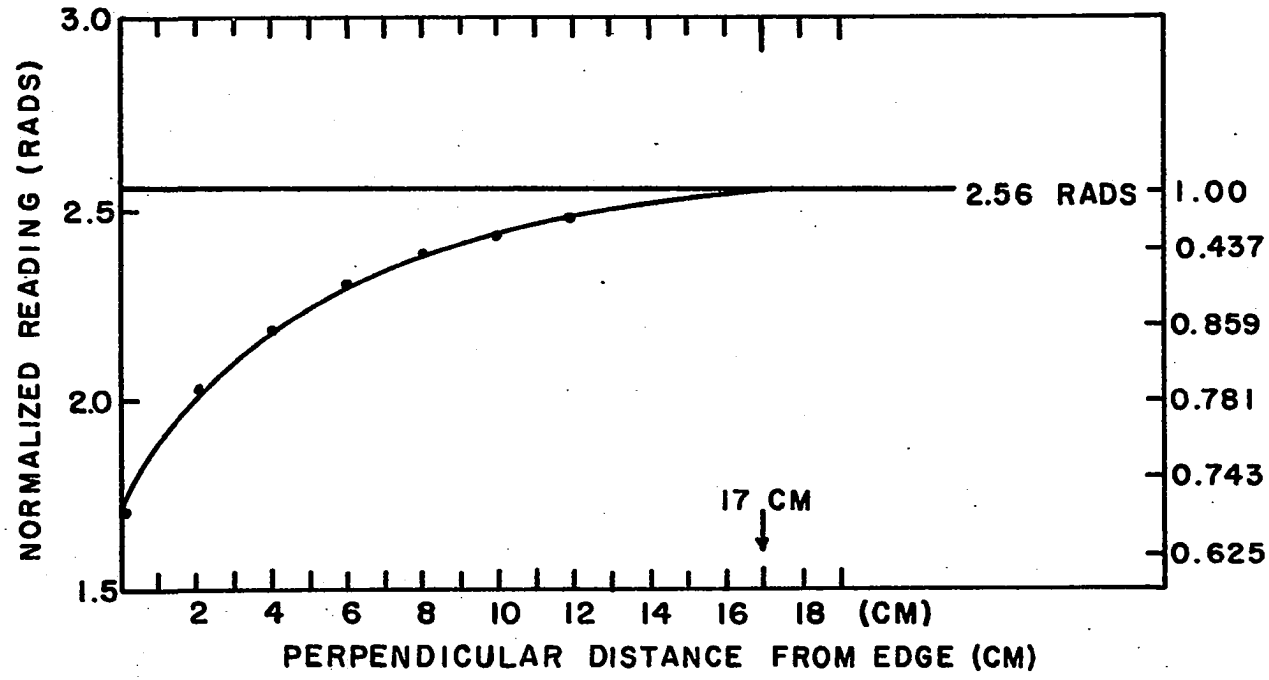

Figure 15. Computer Edge Effect Graph for Cs-137

Table XII. T Distribution Test for Sn-113.

Depth (cm)	mean	Standard Deviation ($x10^{-2}$)	t
½	0.98	10.0	19.34
1	1.01	8.3	21.19
2	1.07	9.8	14.44
3	1.105	8.1	15.33
4	1.16	5.5	17.17
5	1.25	1.4	28.57
6	1.24	3.4	14.29
7	1.275	5.6	4.81
8	1.29	1.4	14.29
9	1.32	1.7	3.03
→ 10	1.34	3.3	1.61
11	1.345	6.4	0.85
12	1.335	1.5	1.67
13	1.305	7.3	1.41
14	1.335	3.7	0.72
15	1.33	2.2	0.49
16	1.32	6.5	0.84
17	1.32	3.1	1.78
18	1.365	5.1	2.45
19	1.325	2.5	2.17

Overall mean = 1.3321 ± 0.040

$t_{.01}(26\text{d.f.}) = 2.479$

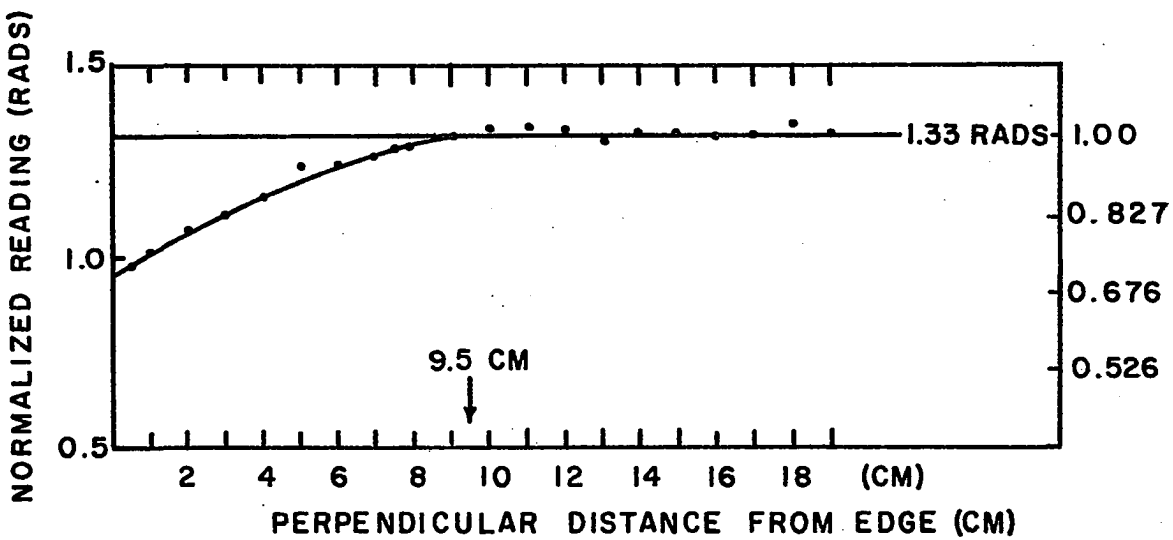

Figure 16. Experimental Edge Effect Graph for Sn-113

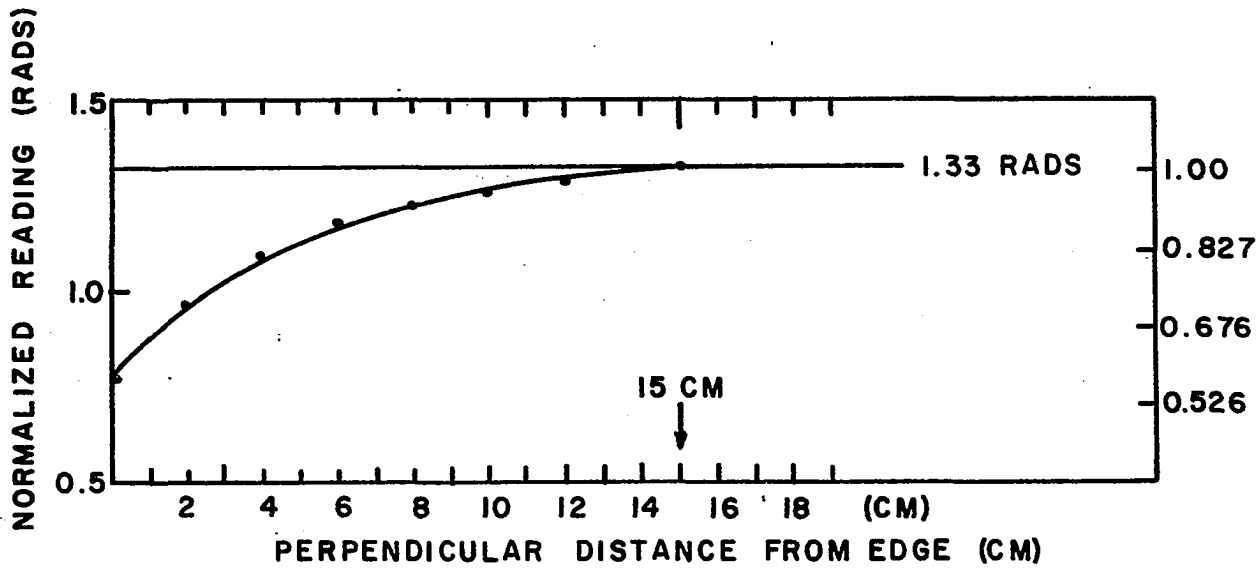

Figure 17. Computer Edge Effect Graph for Sn-113

Table XIII. T Distribution Test for Co-57.

Depth (cm)	mean	Standard Deviation ($x10^{-2}$)	t
½	1.33	17.5	25.86
1	1.55	11.7	28.50
2	1.65	8.6	32.48
3	1.755	8.7	25.16
4	1.87	8.8	17.79
5	1.98	6.8	14.52
6	2.06	6.6	8.20
7	2.03	4.0	17.57
8	2.11	9.8	2.78
→ 9	2.18	10.2	1.07
10	2.16	10.3	0.37
11	2.17	8.1	0.67
12	2.11	4.1	0.65
13	2.13	7.3	2.25
14	2.195	5.0	2.17
15	2.15	5.2	1.05
16	2.18	7.4	1.48
17	2.135	5.2	2.10
18	2.135	5.0	2.17
19	2.22	4.9	2.56

Overall mean = 2.167 ± 0.0348

$t_{.01}(26\text{d.f.}) = 2.479$

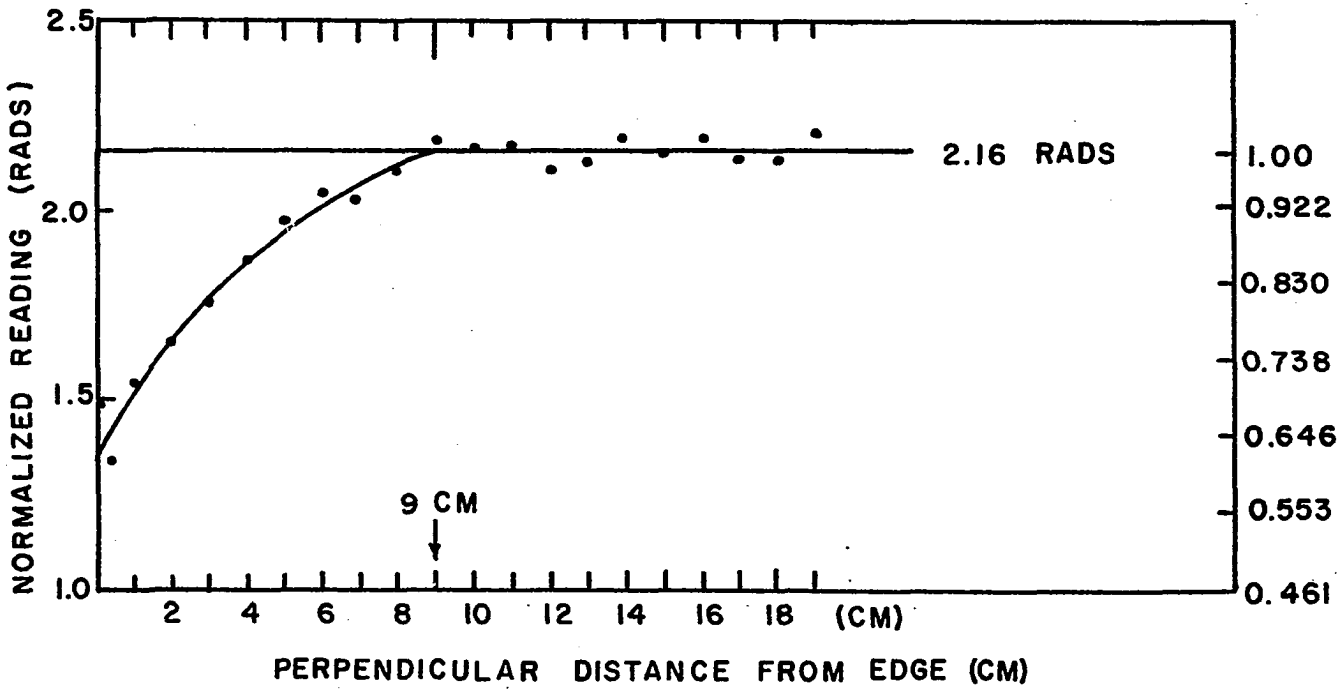

Figure 18. Experimental Edge Effect Graph for Co-57

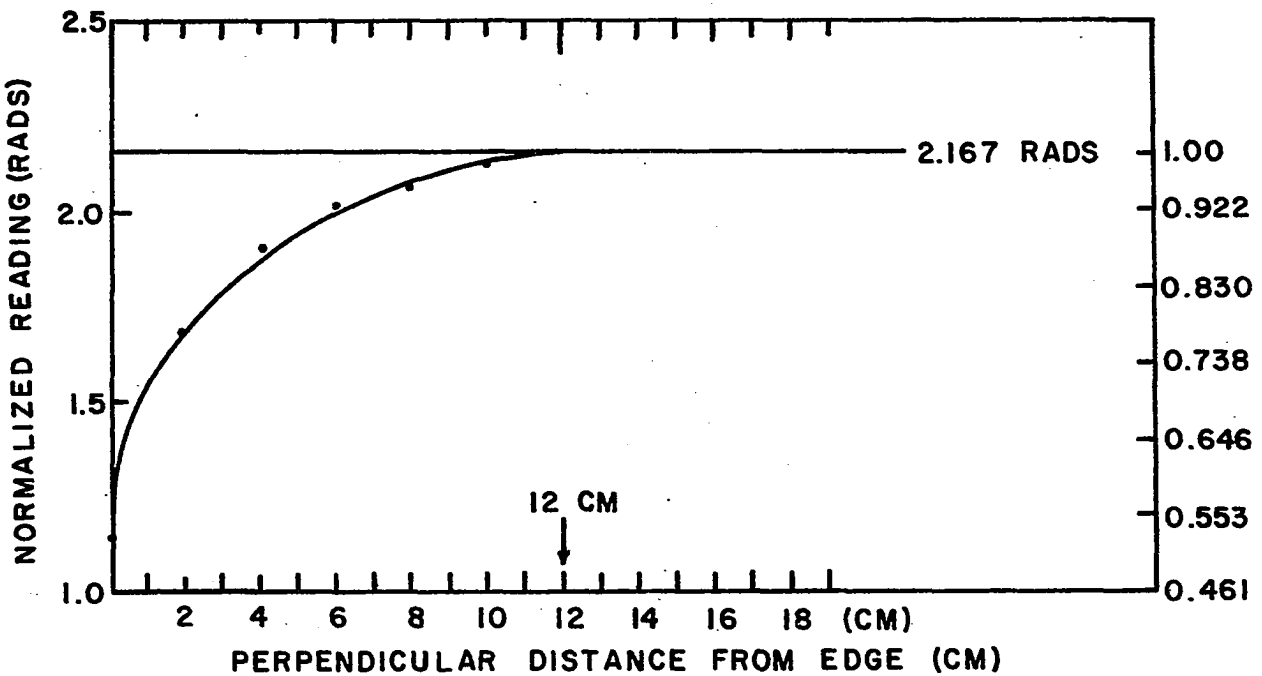

Figure 19. Computer Edge Effect Graph for Co-57